Coalescing binary systems of compact objects to (post)$^{5/2}$-Newtonian order: Late-time evolution and gravitational-radiation emission

Craig W. Lincoln and Clifford M. Will
McDonnell Center for the Space Sciences, Department of Physics, Washington University, St. Louis, Missouri 63130
(Received 20 February 1990)

The late-time evolution of binary systems of compact objects (neutron stars or black holes) is studied using the Damour-Deruelle (post)$^{5/2}$-Newtonian equations of motion with relativistic corrections of all orders up to and including radiation reaction. Using the method of osculating orbital elements from celestial mechanics, we evolve the orbits to separations of $r \approx 2m$, where m is the total mass, at which point the (post)$^{5/2}$-Newtonian approximation breaks down. With the orbits as input, we calculate the gravitational wave form and luminosity using a post-Newtonian formalism of Wagoner and Will. Results are obtained for systems containing various combinations of compact objects, for various values of the mass ratio m_1/m_2, and for various initial values of the orbital eccentricity.

I. INTRODUCTION AND SUMMARY

Binary systems containing compact objects, black holes or neutron stars, which approach a state of coalescence because of gravitational-radiation damping have recently been the focus of increased attention as promising sources of gravitational waves, especially for beam gravitational-wave detectors, such as the proposed Caltech-MIT Laser Interferometric Gravitational Observatory (LIGO). The gravitational waves emitted in the late stages of the evolution of such systems have characteristic amplitudes of $h \approx 10^{-22}$ out to 100 Mpc, and can have frequencies in the kHz range, that increase as the orbital period decreases by virtue of the gravitational-radiation reaction that leads to the coalescence.[1] Strategies have been studied for extracting the characteristic "chirp" signal from noisy data in an array of detectors, and using the signal to obtain such information as the source's direction, its characteristics, and its distance.[2]

As early as 1963, Dyson[3] considered the problem of two coalescing neutron stars, estimating the energy emitted in gravitational waves and the characteristic frequency. The problem was revived by Clark and Eardley,[4] who considered in some detail the effects of tidal disruption, mass stripping, neutrino and gravitational-wave emission, and the frequency of occurrence of such events. The orbital evolution of the system was estimated using Newtonian theory together with the quadrupole approximation for gravitational-wave energy loss. Lattimer and Schramm[5] treated the case of black-hole neutron-star binaries, focusing on the tidal disruption of the neutron star and the ejection of matter into the interstaller medium. Here, the orbital motion was described using the approximation of a test body on a black-hole spacetime, together with a relativistic formalism for analyzing tidal effects.

The rate of occurrence of such coalescences is uncertain, but the estimates are high enough to be interesting. Clark, Van den Heuvel, and Sutantyo[6] estimated three neutron-star binary coalescences per year out to 100–200 Mpc, based on observations in our own Galaxy. The possible formation of dense clusters of neutron stars and stellar mass black holes in galactic nuclei[7] may lead to a number of annual coalescences out to the Hubble distance. A cosmological distribution of binary black holes representing the dark matter has also been proposed,[8] as have supermassive black-hole binaries formed in the coalescence of galactic nuclei.[9] One firm source is known for future observations: the binary pulsar is predicted to decay and coalesce in $\approx 10^8$ yr.[10] In view of the importance of these sources to strategies for gravitational-wave observatories, Thorne[1] has urged that many of these rate estimates be carefully restudied.

Their importance also motivates a careful study of the orbital evolution and gravitational-wave emission from coalescing binaries. One approach to such a study is to use the full machinery of numerical general relativity, together with hydrodynamics, in the case of neutron stars.[11] To date, only limited progress has been made on this front: head-on collisions of black holes and neutron stars have been analyzed,[12] but these are expected to be rare events compared to coalescence following the decay of a binary orbit. Oohara and Nakamura[13] treated coalescing, orbiting neutron stars using a Newtonian three-dimensional (3D) hydrodynamics code, with an initial configuration of two spherical stars in contact. Blackburn and Detweiler[14] studied the late stages of binary orbiting black holes using an approximate initial-value formulation, and a quasistationary assumption. A full numerical treatment of the problem may be several years in the future.

Our approach is to use approximate equations of motion based on an assumption of weak interbody gravitational fields and slow orbital motions, known as the post-Newtonian approximation.[15] However, in order to evolve a binary system as close to coalescence as possible, where the interbody gravitational fields may not be so weak, and where the orbital speeds may not be so small compared to the speed of light, we must use equations of motion carried to the highest practical order of approximation, in order to achieve some measure of reliability. Roughly speaking, the post-Newtonian approximation involves an expansion of the corrections to Newtonian gravitational theory in powers of $\epsilon \approx (m/p) \approx v^2$, where m is the total mass of the binary system, p is a measure of the orbital separation, and v is the orbital velocity. (We use units in which $G = c = 1$.) Schematically, the equations of motion have the form

$$d^2\mathbf{x}/dt^2 = -(m\mathbf{x}/r^3)[1 + O(\epsilon) + O(\epsilon^2) + O(\epsilon^{5/2}) + O(\epsilon^3) + \cdots], \tag{1.1}$$

where $\mathbf{x}$ and $r \equiv |\mathbf{x}|$ are the vector and distance between the two bodies. The first term in square brackets represents the Newtonian acceleration, the second term $O(\epsilon)$ represents the post-Newtonian corrections, the third term $O(\epsilon^2)$ represents the post-post-Newtonian corrections, the fourth term $O(\epsilon^{5/2})$ represents the dominant gravitational-radiation-reaction effects, called $(\text{post})^{5/2}$-Newtonian terms, and so on.

The two-body problem in general relativity has a long and tortuous history,[16] but following the discovery of the binary pulsar in 1974 and the report of apparent gravitational-radiation damping of its orbit in 1978, a systematic effort was made by many groups to obtain approximate two-body equations of motion which included the effects of radiation reaction, which could treat compact objects such as neutron stars as well as noncompact objects, which relied on approximation methods in which the errors could be controlled or estimated, and that were free of *ad hoc* assumptions, such as the use of "point" masses. Of the many different, though equivalent, equations of motion that have emerged from these programs, we have adopted those developed by Damour and Deruelle,[16,17] which contain all the corrections through radiation-reaction $(\text{post})^{5/2}$-Newtonian order in a consistent manner, and which are applicable to neutron stars. With more confidence than rigor, it is believed that they also apply to black holes. The principal restriction is that tidal effects are ignored (the Damour-Deruelle equations also contain terms due to spin, but these are not included in our analysis at present). In the absence of a full 3+1 numerical integration of Einstein's equations, these are the most accurate and self-consistent equations for the evolution of such systems available at present.

We convert the Damour-Deruelle equations of motion to a set of first-order differential equations (Lagrange planetary equations) for the six "osculating orbital elements" that specify the Keplerian orbit that is tangent to the true orbit at the moment in question.[18] Of these, the orbital inclination and angle of ascending node are constant. We evolve the eccentricity e, angle of pericenter ω, and semilatus rectum p [related to the usual semimajor axis by $p \equiv a(1-e^2)$], all the way to zero separation, in principle. The nature of the system being treated determines the point at which we must terminate the evolution.

We have found that, when the post-Newtonian corrections, of order m/p become comparable to the eccentricity e, the osculating element description of the orbit can violate one's Newtonian intuition. For instance, to post-Newtonian order, a circular orbit (r=const) does not correspond to zero eccentricity, instead, is an orbit with fixed e and p, with e and the periastron angle given by

$$e = (3 - \mu/m)m/p + O((m/p)^2), \quad \omega = -\pi + \phi, \tag{1.2}$$

where μ is the reduced mass of the system and ϕ is the orbital phase. Notice that the periastron advances at the *same* rate as the orbit. Thus the system is in a state of "perpetual apastron" ($\phi - \omega = \pi$). To $(\text{post})^{5/2}$-Newtonian order, Eqs. (1.2) are suitably corrected, and p decreases because of radiation reaction. We show that

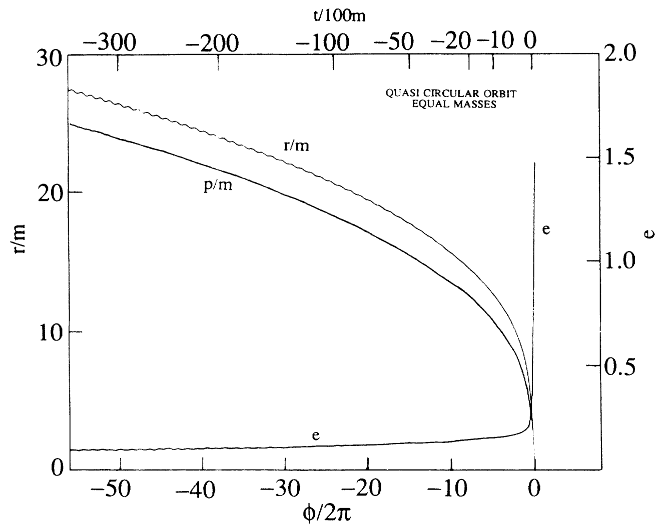

FIG. 1. Evolution of e, p/m, and r/m for equal-mass quasicircular orbit, plotted against $\phi/2\pi \approx$ number of orbits and against time in units of $100m$. Initial condition is $p_i = 25m$. Residual oscillations reflect approximate nature of quasicircular condition for e_i [cf. Eq. (3.5)].

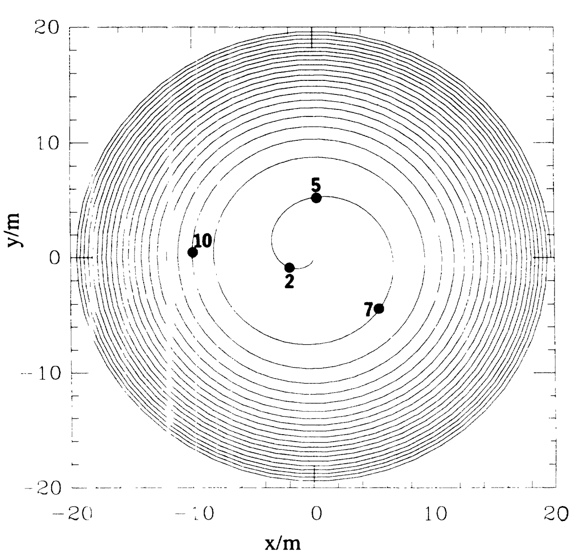

FIG. 2. Quasicircular relative orbit for equal masses. Marked points denote separation in units of m. Around $r = 7m$, orbit enters final "plunge."

any initially noncircular orbit evolves toward such a "quasicircular orbit" on a radiation-reaction time scale.

The effects of the higher post-Newtonian terms are most dramatic for black-hole binary systems, since tidal effects are not expected to be important until the separation is of the order of the sum of the Schwarzschild radii of the holes. (In the harmonic coordinate system which we use, the Schwarzschild radius is m instead of $2m$.) For a quasicircular orbit of two equal-mass black holes, for example, with $p \approx 25m$ initially, the evolution of r and e and of the relative orbit are shown in Figs. 1 and 2. At a separation of around $7m$, the bodies enter a final orbit in which they "plunge" toward each other.

The gravitational radiation emitted by the system is determined using the post-Newtonian gravitational wave forms derived by Wagoner and Will,[19] which contain the leading "quadrupole formula" terms, and the first post-Newtonian corrections thereto. By analogy with Eq. (1.1), these wave forms have the schematic form

$$h_{ij}=(2\mu/R)[O(\epsilon)+O(\epsilon^{3/2})+O(\epsilon^2)+\cdots] , \quad (1.3)$$

where R is the distance between the observer and the binary system. Although these formulas are formally not as accurate as the orbit, we expect them to give a good semiquantitative picture of the radiation, and of the secular evolution of the wave-form shape and frequency. Figure 3(a) illustrates the $\times$ polarization gravitational wave form emitted along the orbital axis by the evolution of Figs. 1 and 2. The changing frequency of the wave form, leading to the characteristic "chirp" signal, can be seen. The gravitational luminosity is also obtained from the Wagoner-Will post-Newtonian formalism. Approximately 0.3% of the rest mass of the system is emitted by the time the separation has reached $9m$ where the approximation for the luminosity was deemed to break down. We also study the evolution and radiation from a quasi-

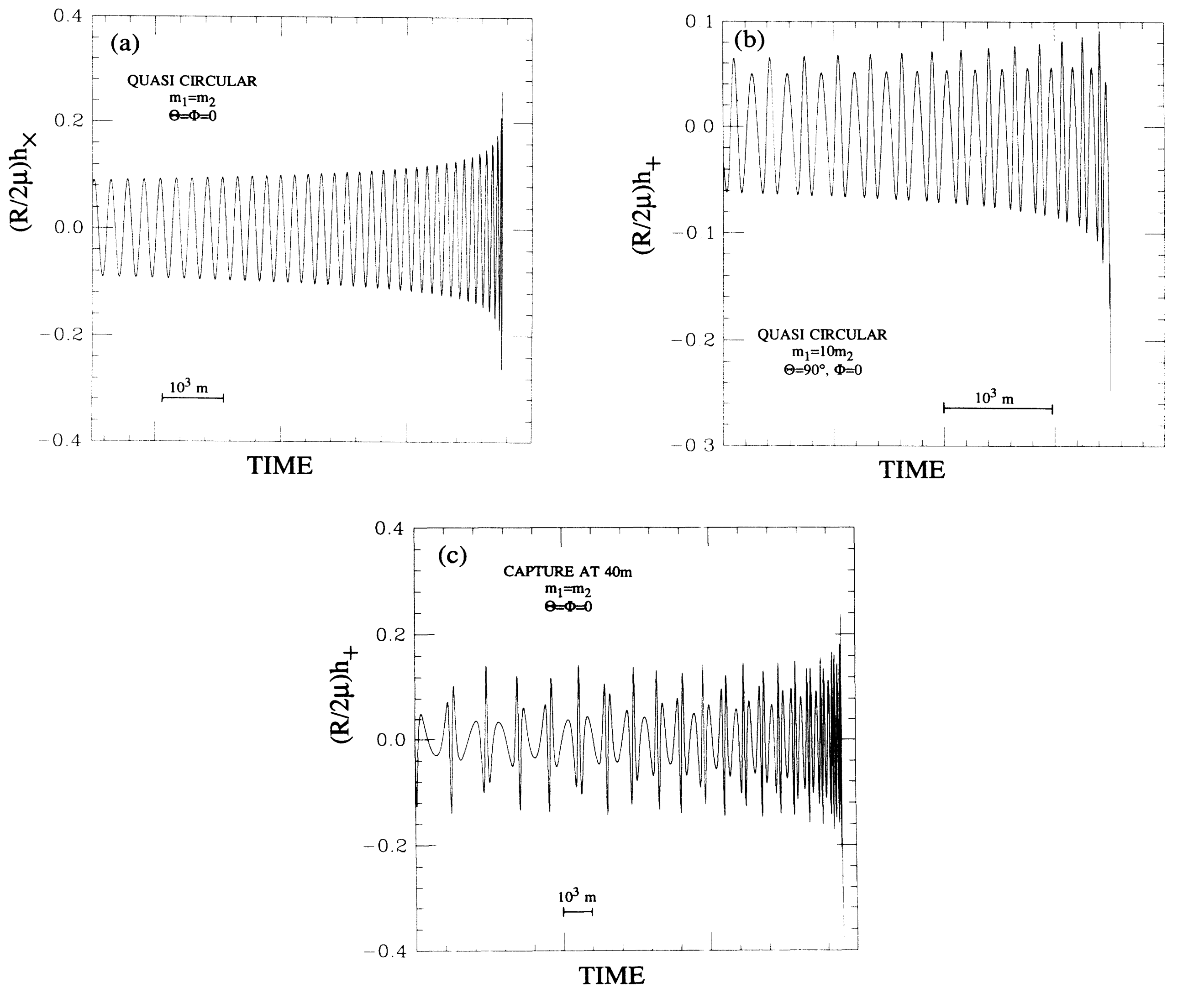

FIG. 3. Gravitational wave forms from coalescing binaries. Plotted is $(R/2\mu)h$ against time. Growing amplitude and increasing frequency are evident. (a) Cross ($\times$) polarization along orbit axis for equal-mass quasicircular orbit. (b) Plus (+) polarization in orbital plane for $m_1=10m_2$ quasicircular orbit. (c) Plus polarization along orbit axis for equal-mass capture into an $e_i=1$ orbit with $p_i=40m$. Short bursts are emitted when system is at apastron; evolving interburst shape reflects rapid advance of periastron relative to line of sight.

circular orbit of two bodies with the mass ratio 10:1. The corresponding wave form is shown in Fig. 3(b). Figure 3(c) shows the wave form of the late decay of a system of two equal masses which has been captured into an eccentric orbit through gravitational-radiation damping, with an initial value of p of about $40m$. The effect of the eccentricity is seen in the structure of the wave form.

The remainder of this paper provides the details of the method and further results. In Sec. II we summarize the Damour-Deruelle $(\text{post})^{5/2}$-Newtonian equations of motion and the Wagoner-Will post-Newtonian gravitational wave-form formalism, and evaluate the importance of tidal effects. Section III treats the evolution of the orbits and Sec. IV treats the gravitational radiation emitted. Section V contains concluding remarks. In Appendix A we study in detail the evolution of generic orbits toward the quasicircular state described by Eq. (1.2), and in Appendix B we estimate the effect of tidal dissipation in black holes.

II. BASIC EQUATIONS FOR ORBITAL MOTION AND GRAVITATIONAL RADIATION

A. Damour-Deruelle equations of motion

We adopt the equations of motion for two condensed bodies with all contributions up to and including the $(\text{post})^{5/2}$ Newtonian, or radiation-reaction terms, developed by Damour and Deruelle.[16,17] They can be written schematically as

$$\begin{aligned}\mathbf{a}_1 &\equiv d^2\mathbf{x}_1/dt^2\\ &= -(m_2/r^2)\mathbf{n}\\ &\quad +(m_2/r^2)\{\mathbf{n}[(PN)+(P^2N)+(P^{5/2}N)]\\ &\qquad +\mathbf{v}[(PN)+(P^2N)+(P^{5/2}N)]\}\ , \end{aligned} \tag{2.1}$$

where $\mathbf{n}$ is the unit vector from body 2 to body 1, r is the separation, and $\mathbf{v}$ is the relative velocity. The leading term is the usual Newtonian contribution, and the post-Newtonian and higher contributions are represented by the notation P^mN. The equation for $\mathbf{a}_2$ is found by interchanging subscripts 1 and 2 and changing the sign of $\mathbf{n}$ and $\mathbf{v}$ in the equation for $\mathbf{a}_1$.

These equations are an expansion in the small parameter $\epsilon \approx v^2 \approx m/r$. As this parameter approaches unity the equations become invalid. Furthermore, the derivation of the equations assumed that tidal interactions could be ignored, so that there is an "effacement" of the internal structure of the bodies, whose consequence is that their motions depend only on their masses. However, as the bodies approach each other, tidal effects will play a role. These effects are discussed in Sec. II D. The Damour-Deruelle equations do include terms involving the spin of the bodies, but those terms also do not become important until the bodies are close to each other. Thus we shall treat the idealized problem of two effaced compact masses in mutual orbit and will evolve the system, at least formally, to infinitesimal separation. When we apply the results of our idealized analysis to real systems, we shall cut the evolution off at states, which depend on the nature of the two bodies, beyond which tidal effects must be included or the approximation breaks down.

To discuss the expected accuracy of these equations in describing coalescing binaries, we must distinguish between dissipative and nondissipative effects. The even-order post-Newtonian corrections in Eq. (2.1) produce nondissipative effects, such as periodic perturbations of the Newtonian orbit. Since the P^2N correction is included, the errors are of order ϵ^3. (These terms also produce nondissipative, but secular effects, such as the periastron advance, but these are not central to the present discussion.) The odd-half order terms, such as the $P^{5/2}N$ terms, produce damping. Over an orbital time scale, these terms produce corrections of order $\epsilon^{5/2}$, but since they are secular, they can ultimately produce a deviation from the initial fixed Newtonian orbit that is of order unity, if integrated over a dissipative time scale proportional to $\epsilon^{-5/2}$. Therefore, although formally the error in the dissipative term in the equation of motion is of order $\epsilon^{7/2}$ (the first odd-half-order term ignored), the *relative* error in such damped quantities as the orbital separation after a dissipation time scale will be of order ϵ.

We now convert the two-body equations of motion (2.1) to an effective one-body problem. From the Damour-Deruelle equations one can derive an integral of the motion[20] to post-post-Newtonian order, which can be taken as the center of mass of the system. Choosing a coordinate system with its origin at this center of mass, we can change variables to a "relative" coordinate $\mathbf{x}\equiv\mathbf{x}_1-\mathbf{x}_2$ using the equations

$$\begin{aligned}\mathbf{x}_1 &= [m_2/m+(\eta\,\delta m/2m)(v^2-m/r)]\mathbf{x}\ ,\\ \mathbf{x}_2 &= [-m_1/m+(\eta\,\delta m/2m)(v^2-m/r)]\mathbf{x}\ ,\end{aligned} \tag{2.2}$$

where we define $m\equiv m_1+m_2$, $\mu\equiv m_1m_2/m$, $\delta m=m_1-m_2$, $\eta\equiv\mu/m$, $r\equiv|\mathbf{x}|$, $\mathbf{x}\equiv r\mathbf{n}$, $\mathbf{v}\equiv\mathbf{v}_1-\mathbf{v}_2$.

For our purposes, only the post-Newtonian corrections are needed in Eqs. (2.2), since the Newtonian acceleration is automatically expressed in terms of $\mathbf{x}$, and the change of variables is needed only in post-Newtonian and higher terms. By taking a time derivative of Eqs. (2.2) and using the Newtonian equations of motion in any post-Newtonian terms, one can obtain analogous transformations for the velocities.

Using the transformations defined above, we obtain the relative acceleration

$$\mathbf{a}\equiv\mathbf{a}_1-\mathbf{a}_2=(m/r^2)[(-1+A)\mathbf{n}+B\mathbf{v}]\ , \tag{2.3}$$

where A and B represent post-, post-post-, and $(\text{post})^{5/2}$-Newtonian correction terms. Writing $A\equiv A_1+A_2+A_{5/2}$ and $B\equiv B_1+B_2+B_{5/2}$, we have

$$A_1=2(2+\eta)\frac{m}{r}-(1+3\eta)v^2+\frac{3}{2}\eta\dot{r}^2\ , \tag{2.4a}$$

$$\begin{aligned}A_2 &= -\frac{3}{4}(12+29\eta)\left[\frac{m}{r}\right]^2-\eta(3-4\eta)v^4\\ &\quad -\frac{15}{8}\eta(1-3\eta)\dot{r}^4+\frac{3}{2}\eta(3-4\eta)v^2\dot{r}^2\\ &\quad +\frac{1}{2}\eta(13-4\eta)\frac{m}{r}v^2+(2+25\eta+2\eta^2)\frac{m}{r}\dot{r}^2\ ,\end{aligned} \tag{2.4b}$$

$$A_{5/2}=\frac{8}{5}\eta\frac{m}{r}\dot{r}\left[3v^2+\frac{17}{3}\frac{m}{r}\right] , \tag{2.4c}$$

$$B_1=2(2-\eta)\dot{r} , \tag{2.4d}$$

$$B_2=\frac{1}{2}\dot{r}\left[\eta(15+4\eta)v^2-(4+41\eta+8\eta^2)\frac{m}{r}\right.$$
$$\left.-3\eta(3+2\eta)\dot{r}^2\right] , \tag{2.4e}$$

$$B_{5/2}=-\frac{8}{5}\eta\frac{m}{r}\left[v^2+3\frac{m}{r}\right] , \tag{2.4f}$$

where an overdot denotes d/dt.

B. Osculating orbit elements and the Lagrange planetary equations

Viewing this as a Newtonian orbital problem with perturbations suggests using the method of osculating orbital elements from celestial mechanics[18] (for a description in terms of an alternative set of orbit elements, see Ref. 21). The basic picture is the following: at any given instant one can find a Keplerian orbit that is "tangent" to the true orbit in the sense that the position and velocity of the particle on the true orbit coincide with the position and velocity of the tangent Keplerian orbit at that moment. Such a Keplerian orbit is called an "osculating orbit." At a subsequent instant the actual orbit will, in general, be tangent to a different Keplerian orbit. Thus, as time advances, the orbital elements for the osculating orbit will change smoothly.

A general Keplerian two-body orbit is uniquely specified by six parameters (see Fig. 4): i, the inclination of the orbit relative to a reference plane, Ω, the angle to the line of ascending node, ω, the angle between the line of node and the pericentric line, a, the semimajor axis e, the eccentricity, and T, the time of pericentric passage.

The position and velocity are then found from the definitions

$$x'\equiv r\cos\psi , \tag{2.5a}$$

$$y'\equiv r\sin\psi , \tag{2.5b}$$

$$z'\equiv 0 , \tag{2.5c}$$

$$p/r\equiv 1+e\cos(\psi-\omega) , \tag{2.5d}$$

$$\dot{r}\equiv(m/p)^{1/2}e\sin(\psi-\omega) , \tag{2.5e}$$

$$r^2\dot{\psi}\equiv(mp)^{1/2} , \tag{2.5f}$$

where ψ is the angle in the orbit from the ascending node, $p\equiv a(1-e^2)$, and the relations between the primed and unprimed coordinates in terms of i and Ω are

$$\begin{aligned} x&\equiv x'\cos\Omega-y'\sin\Omega\cos i+z'\sin\Omega\sin i , \\ y&\equiv x'\sin\Omega+y'\cos\Omega\cos i-z'\cos\Omega\sin i , \\ z&\equiv y'\sin i+z'\cos i . \end{aligned} \tag{2.6}$$

If we now view these equations as a change of variables from **x** and **v** to i, Ω, ω, a, e, and T and substitute into the original perturbed problem, we find a set of equations for the time derivatives of the osculating orbital elements, called the Lagrange planetary equations. Resolving the perturbing acceleration into a radial component R, a component S perpendicular to R and in the direction of advancing ψ, and the component W, perpendicular to the orbital plane, we can rewrite the Lagrange planetary equations as

$$di/dt=\frac{r\cos\psi}{(mp)^{1/2}}W , \tag{2.7a}$$

$$\dot{\Omega}=\frac{r\sin\psi}{(mp)^{1/2}\sin i}W , \tag{2.7b}$$

$$\dot{a}=\frac{2a^2}{(mp)^{1/2}}[eR\sin(\psi-\omega)+(p/r)S] , \tag{2.7c}$$

$$\dot{e}=(p/m)^{1/2}\{R\sin(\psi-\omega)$$
$$+[e(r/p)+(1+r/p)\cos(\psi-\omega)]S\} , \tag{2.7d}$$

$$e\dot{\omega}=(p/m)^{1/2}[-R\cos(\psi-\omega)+(1+r/p)\sin(\psi-\omega)S$$
$$-e(r/p)\cot i\sin(\psi-\omega)W] , \tag{2.7e}$$

$$m\dot{T}=a[2r-(p/e)\cos(\psi-\omega)$$
$$-3(m/p)^{1/2}e(t-T)\sin(\psi-\omega)]R$$
$$+(a/e)[(r+p)\sin(\psi-\omega)$$
$$-3(mp)^{1/2}e(t-T)/r]S . \tag{2.7f}$$

Notice that $\dot{\omega}$ can becomes singular for $e=0$. This problem can be avoided by making the change of variables $\alpha=e\cos\omega$, $\beta=e\sin\omega$ and determining the evolution of α and β.

In the problem considered here, the perturbing acceleration is a linear combination of **n** and **v**, so that $W=0$, and the orbital plane is fixed ($di/dt=d\Omega/dt=0$). We therefore choose the orbital plane to be the x-y plane

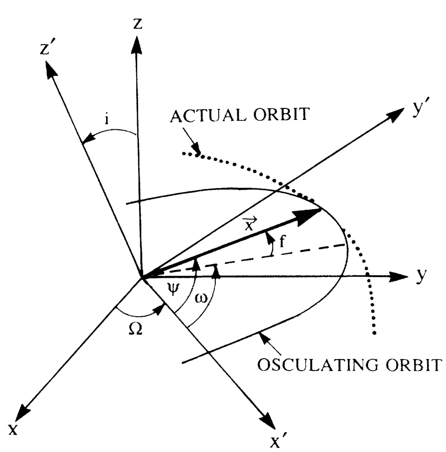

FIG. 4. Osculating orbit elements. Orientation of osculating orbit in space is determined by i, Ω, and ω. In orbital plane, osculating ellipse is determined by a and e.

and the line of nodes to be the x axis. We then have $\psi=\phi$ (ϕ is the usual polar angle), and the definitions

$$\mathbf{x}\equiv r(\mathbf{e}_x\cos\phi+\mathbf{e}_y\sin\phi)\ , \tag{2.8a}$$

$$\mathbf{v}\equiv(m/p)^{1/2}[-\mathbf{e}_x(\sin\phi+e\sin\omega)+\mathbf{e}_y(\cos\phi+e\cos\omega)]\ , \tag{2.8b}$$

$$p/r\equiv 1+e\cos f\ , \tag{2.8c}$$

$$\dot r\equiv(m/p)^{1/2}e\sin f\ , \tag{2.8d}$$

$$r^2\dot\phi\equiv(mp)^{1/2}\ , \tag{2.8e}$$

where $f\equiv\phi-\omega$. In addition we have $R=(m/r^2)(A+\dot rB)$ and $S=(m/r)\dot\phi B$.

With the use of Eq. (2.8e) for $\dot\phi$ to change dependent variables, our Lagrange planetary equations are then

$$\frac{d(a/m)}{d\phi}=2\left[\frac{a}{m}\right]^2\frac{m}{p}\left[eA\sin f+\left[\frac{m}{p}\right]^{1/2}B(1+e^2+2e\cos f)\right]\ , \tag{2.9a}$$

$$\frac{de}{d\phi}=A\sin f+2\left[\frac{m}{p}\right]^{1/2}B(e+\cos f)\ , \tag{2.9b}$$

$$e\frac{d\omega}{d\phi}=-A\cos f+2\left[\frac{m}{p}\right]^{1/2}B\sin f\ , \tag{2.9c}$$

or the equivalent set

$$\frac{d(p/m)}{d\phi}=2\left[\frac{p}{m}\right]^{1/2}B\ , \tag{2.10a}$$

$$\frac{d\alpha}{d\phi}=A\sin\phi+2\left[\frac{m}{p}\right]^{1/2}B(\alpha+\cos\phi)\ , \tag{2.10b}$$

$$\frac{d\beta}{d\phi}=-A\cos\phi+2\left[\frac{m}{p}\right]^{1/2}B(\beta+\sin\phi)\ . \tag{2.10c}$$

Since the time of pericentric passage T amounts to an initial choice of time, we shall not consider it further.

When the definitions of $\mathbf{x}$ and $\mathbf{v}$ [Eqs. (2.8)] are substituted into the expressions for A and B, these equations become coupled first-order differential equations for the variables e, ω, and p, given by

$$\begin{aligned}\frac{de}{d\phi}=\frac{m}{p}&\left[(3-\eta)\sin f+(5-4\eta)e\sin 2f+\frac{e^2}{8}[(56-47\eta)\sin f-3\eta\sin 3f]\right]\\&-\left[\frac{m}{p}\right]^2\left[\tfrac{1}{4}(36+73\eta-8\eta^2)\sin f+(11+31\eta-3\eta^2)e\sin 2f\right.\\&\quad+\frac{e^2}{16}[(60+245\eta-64\eta^2)\sin 3f+(92+181\eta-32\eta^2)\sin f]\\&\quad+\frac{e^3}{8}[(2+25\eta-16\eta^2)\sin 4f+4(3-11\eta-10\eta^2)\sin 2f]\\&\quad\left.+\frac{\eta}{128}e^4[15(1-3\eta)\sin 5f-3(73+53\eta)\sin 3f-2(477+161\eta)\sin f]\right]\\&-\frac{\eta}{15}\left[\frac{m}{p}\right]^{5/2}[192\cos f+16e(19+20\cos 2f)+2e^2(91\cos 3f+269\cos f)\\&\quad+e^3(121+180\cos 2f+35\cos 4f)+6e^4(3\cos 3f+5\cos f)]\ ,\end{aligned} \tag{2.11a}$$

$$\begin{aligned}e\frac{d\omega}{d\phi}=\frac{m}{p}&\left[-(3-\eta)\cos f+e[3-(5-4\eta)\cos 2f]+\frac{e^2}{8}[3\eta\cos 3f+(8+21\eta)\cos f]\right]\\&+\left[\frac{m}{p}\right]^2\left[\tfrac{1}{4}(36+73\eta-8\eta^2)\cos f+e[(7+5\eta-7\eta^2)+(11+31\eta-3\eta^2)\cos 2f]\right.\\&\quad+\frac{e^2}{16}[(84+79\eta-224\eta^2)\cos f+(60+245\eta-64\eta^2)\cos 3f]\\&\quad+\frac{e^3}{8}[(2+25\eta-16\eta^2)\cos 4f-2\eta(1+24\eta)\cos 2f-(2-21\eta+48\eta^2)]\\&\quad\left.+\frac{\eta}{128}e^4[15(1-3\eta)\cos 5f+3(33-19\eta)\cos 3f+10(27-41\eta)\cos f]\right]\\&-\frac{\eta}{15}\left[\frac{m}{p}\right]^{5/2}[192\sin f+320e\sin 2f+2e^2(91\sin 3f+115\sin f)\\&\quad+5e^3(7\sin 4f+26\sin 2f)+18e^4(\sin 3f+\sin f)]\ ,\end{aligned} \tag{2.11b}$$

$$\frac{d(p/m)}{d\phi}=4(2-\eta)e\sin f$$
$$+e\frac{m}{p}[-2(2+13\eta+2\eta^2)\sin f-\tfrac{1}{2}(4+11\eta)e\sin 2f+\tfrac{1}{4}\eta(33-2\eta)e^2\sin f+\tfrac{3}{4}\eta(3+2\eta)e^2\sin 3f]$$
$$-\frac{8}{5}\eta\left[\frac{m}{p}\right]^{3/2}(8+18e\cos f+7e^2+5e^2\cos 2f+2e^3\cos f)\ . \qquad (2.11c)$$

(The equivalent set of equations for α and β are given in Appendix A.) Given a solution for these variables, one can then integrate Eq. (2.8e) to determine ϕ as a function of time. The solution can then be substituted back into the definitions (2.8) to obtain the motion of the system.

C. Post-Newtonian gravitational wave forms

Once we know the motion of the system as a function of time we can determine the gravitational wave form and the gravitational luminosity. An observer at a distance R from a binary system in the x-y plane will see the two polarization states h_+ and $h_\times$ of the gravitational radiation wave form given by[22]

$$h_+\equiv h_{\mathrm{TT}}{}^{\Theta\Theta}\equiv -h_{\mathrm{TT}}{}^{\Phi\Phi}=\tfrac{1}{4}(1+\cos^2\Theta)[\cos 2\Phi(h^{xx}-h^{yy})+2\sin 2\Phi h^{xy}]-\tfrac{1}{4}\sin^2\Theta(h^{xx}+h^{yy})\ , \qquad (2.12a)$$

$$h_\times\equiv h_{\mathrm{TT}}{}^{\Theta\Phi}\equiv h_{\mathrm{TT}}{}^{\Phi\Theta}=\cos\Theta[\cos 2\Phi h^{xy}-\tfrac{1}{2}\sin 2\Phi(h^{xx}-h^{yy})]\ , \qquad (2.12b)$$

where Θ and Φ determine the observation direction, and TT denotes the transverse traceless part.

For h^{ij} we use the post-Newtonian formulas developed by Wagoner and Will.[19] These are based on the Epstein-Wagoner formalism[23] which gives a post-Newtonian expansion for the far-zone metric perturbation h^{ij} in terms of time derivatives of integrals over the near zone of the stress-energy distribution (the boundary between the far zone and the near zone is a region of size given by the wavelength of the gravitational waves). Assuming an effective point-mass model (nonrotating perfect-fluid balls with negligible tidal effects), Wagoner and Will obtained the post-Newtonian formula

$$h^{ij}_{\mathrm{TT}}=(2\mu/R)(2(v^iv^j-mx^ix^j/r^3)+(\delta m/m)[3(\mathbf{N}\cdot\mathbf{x})(m/r^3)(2v^{(i}x^{j)}-\dot r x^ix^j/r)-(\mathbf{N}\cdot\mathbf{v})(2v^iv^j-mx^ix^j/r^3)]$$
$$+\tfrac{1}{3}(1-6\eta)(m/r)[2v^iv^j-(x^ix^j/r^2)(2\tilde E+3m/r-3\dot r^2)-4v^{(i}x^{j)}\dot r/r]$$
$$+2\{(1-3\eta)v^iv^j\tilde E-(mx^ix^j/r^3)[3(1+\eta)\tilde E-(2-4\eta)m/r-\tfrac{3}{2}\eta\dot r^2]+(4-2\eta)v^{(i}x^{j)}m\dot r/r^2\}$$
$$+(1-3\eta)\{2(\mathbf{N}\cdot\mathbf{v})^2(v^iv^j-\tfrac{1}{3}mx^ix^j/r^3)-\tfrac{4}{3}(\mathbf{N}\cdot\mathbf{v})(\mathbf{N}\cdot\mathbf{x})(m/r^3)(8v^{(i}x^{j)}-3\dot r x^ix^j/r)$$
$$-\tfrac{1}{3}(\mathbf{N}\cdot\mathbf{x})^2(m/r^3)[14v^iv^j-(x^ix^j/r^2)(6\tilde E+13m/r-15\dot r^2)-30v^{(i}x^{j)}\dot r/r]\})_{\mathrm{TT}}\ , \qquad (2.13)$$

where $\mathbf{N}$ is a unit vector toward the observation direction, and where

$$\tilde E=\tfrac{1}{2}v^2-m/r+O(\epsilon^4)\ . \qquad (2.14)$$

The luminosity is given by

$$L=\tfrac{8}{15}(\mu^2m^2/r^4)\{(12v^2-11\dot r^2)+24(\tilde E+m/r)[14\eta\tilde E-(6-9\eta)m/r]$$
$$-2\dot r^2[2(33+43\eta)\tilde E+3(8+21\eta)m/r-\tfrac{3}{2}(20+3\eta)\dot r^2]$$
$$+4(1-6\eta)[(\tilde E+m/r)(6\tilde E+7m/r)-\tfrac{1}{3}\dot r^2(21\tilde E+23m/r-6\dot r^2)]$$
$$+\tfrac{1}{7}(1-3\eta)[16(\tilde E+m/r)(17\tilde E-10m/r)-\tfrac{1}{3}\dot r^2(144\tilde E-440m/r+105\dot r^2)]$$
$$+\tfrac{1}{7}(1-4\eta)[(\tilde E+m/r)(345\tilde E+397m/r)+4(m/r)^2-\dot r^2(319\tilde E+349m/r-297\dot r^2/4)]\}\ . \qquad (2.15)$$

Equivalent formulas have been obtained by Blanchet and Schäfer.[24] The Wagoner-Will wave form contains only the first post-Newtonian correction beyond the dominant quadrupole contribution, thus in some sense the formula is not as accurate as the orbit, which is valid through 5/2 orders beyond Newtonian theory. Nevertheless, it is an improvement over the simple quadrupole expression, and therefore we shall use it to give a better, though limited approximation to the gravitational wave form and luminosity from the coalescing system.

D. Tidal effects and termination of the evolution

There are three kinds of tidal gravitational effects to be considered in determining the extent of validity of the

Damour-Deruelle equations: tidal stripping and disruption (for neutron stars), orbital tidal effects, and tidal dissipation.

When tidal forces are sufficient to strip matter from one of the component stars, the orbital evolution can change dramatically. For instance, mass transfer can cause the orbital separation to increase, despite the dissipative effect of gravitational radiation. Similarly, if one of the stars is completely disrupted, hydrodynamics will play an important role. Therefore, for systems of two neutron stars or of a neutron star and a black hole, the separation at which this occurs marks an obvious termination point for our purely gravitational evolution. A useful approximation to this "stripping distance," r_S is given by the separation at which the Roche radius of one of the stars equals its physical radius R. For the star labeled 2 this is given approximately by[25]

$$r_S \approx \frac{3^{4/3}}{2} R \left[1+\frac{m_1}{m_2} \right]^{1/3} . \qquad (2.16)$$

Substituting $R \approx 11$ km, a characteristic neutron-star radius for masses in the range 0.5 to $1.5 M_\odot$ we find that for various masses, the stripping distances estimated from Eq. (2.16) agree within 10% with those determined by Clark and Eardley from numerical simulations.[4] Equation (2.16) can be rewritten in the form

$$\frac{r_S}{m} \approx 10 \left[\frac{M_\odot}{m_2} \right] [\tfrac{1}{2}(1+X)]^{-2/3} \qquad (2.17)$$

where $X \equiv m_1/m_2$. Figure 5 plots values of r_S/m against m_2 for various mass ratios. For two neutron stars of $1.4 M_\odot$ each, the minimum separation is about $7m$.

Tidal interactions produce orbital perturbations which compete with the post-Newtonian effects which we are studying. One way to estimate their importance is to consider the additional periastron advance produced by the mutual tidal deformation of two bodies. The advance per orbit is given approximately by[26]

$$\Delta\omega \approx 30\pi \left[k_2 \left[\frac{m_1}{m_2} \right] \left[\frac{R_2}{p} \right]^5 + k_1 \left[\frac{m_2}{m_1} \right] \left[\frac{R_1}{p} \right]^5 \right] , \qquad (2.18)$$

where k_i is the "apsidal-motion constant" for each star, having representative values of 0.1 for polytropes of index 5/3, and 0.75 for homogeneous stars. We have ignored a factor of order unity dependent upon the orbital eccentricity. If we adopt as the point of termination of the orbit that separation at which the tidal periastron advance is comparable to the post-post-Newtonian contribution, given roughly by $\Delta\omega_{PPN} \approx 6\pi(m/p)^2$, we obtain a minimum separation for two neutron stars given by

$$\left[\frac{p}{m} \right]_{\rm min} \sim 5 \left[\frac{k}{0.1} \right]^{1/3} \left[\frac{R}{11\ {\rm km}} \right]^{5/3} \times \left[\frac{m}{2.8 M_\odot} \right]^{-5/3} \left[\frac{X+X^{-1}}{2} \right]^{1/3} , \qquad (2.19)$$

with a comparable result for one neutron star and one black hole. This is smaller than the stripping distance for most systems of interest. For two black holes, tidal effects are smaller, since $R_H = m_H$, and $k_H \leq 1$, so that the resulting minimum separation is given by

$$\left[\frac{p}{m} \right]_{\rm min} \sim 1.4 k_H^{1/3} \left[\frac{X(1+X)^3)}{12(1+X)^5} \right]^{1/3} , \qquad (2.20)$$

where the quantity in square brackets is smaller than unity.

The third effect of tidal interactions is tidal dissipation, which competes with the gravitational-radiation reaction (see also Ref. 27). For bodies with rotation axes normal to the plane of the orbit, and for a circular orbit, the rate of change of the orbital period due to tidal dissipation is given by[28]

$$\left[\frac{\dot P}{P} \right]_T \simeq \frac{672\pi}{25} \left[\frac{m m_1}{m_2^2} \left[\frac{R_2}{p} \right]^8 \left[\frac{R_2 \langle \eta_2 \rangle}{m_2} \right] \times (1-\Omega_2/n) + (2 \leftrightarrow 1) \right] , \qquad (2.21)$$

where $n \equiv 2\pi/P$ is the orbital mean motion, Ω is the angular velocity of the body, and $\langle \eta \rangle$ is an average coefficient of viscosity given by

$$\langle \eta \rangle = (9/R^9) \int_0^R \eta r^8 dr , \qquad (2.22)$$

where η is the local coefficient of viscosity in units of $\mathrm{g\,cm^{-1} s^{-1}}$. The gravitational-radiation reaction in a circular orbit gives[29]

$$\dot P/P = \tfrac{96}{5} \mu m^2/p^4 . \qquad (2.23)$$

These effects will be comparable when

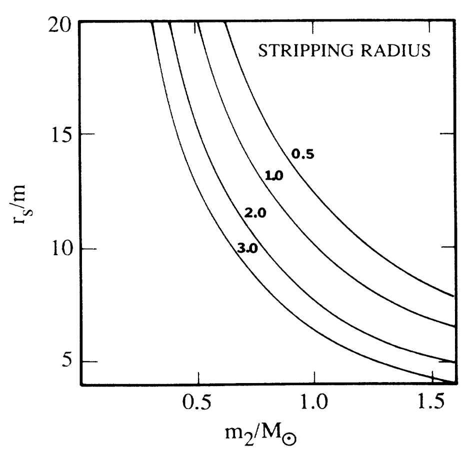

FIG. 5. Stripping radius, at which Roche radius of star of mass m_2 equals its physical radius; for smaller separations tidal stripping or disruption of star will occur. Curves are labeled by mass ratio $X = m_1/m_2$. For comparable-mass neutron stars of $1.4\ M_\odot$ each, stripping radius is around $7m$.

$$\left[\frac{p}{m}\right]_{\min} \simeq 7\times 10^{-8}\left[\frac{R}{11\ \mathrm{km}}\right]^{9/4}\left[\frac{m}{2.8M_\odot}\right]^{-2} \times(1+X)[\langle \eta_2\rangle(1-\Omega_2/n) + X^{-4}\langle \eta_1\rangle(1-\Omega_1/n)]^{1/4} . \qquad (2.24)$$

For neutron stars Eq. (2.22) shows that $\langle \eta \rangle$ will be dominated by dissipative processes in the crust of the star, where the density is less than 2×10^{14} g cm^{-3}; calculations of the viscosity for densities in this regime (in the absence of magnetic fields) yield[30] $\eta < 10^{19}$, so that viscous damping is always negligible compared to gravitational-radiation damping.

For slowly rotating black holes, the effective coefficient of viscosity is $\langle \eta_i \rangle = \alpha / m_i$, where $\alpha \approx 5/7\pi$ (see Appendix B). In this case, tidal and gravitational-radiation dissipation will be comparable when

$$\left[\frac{p}{m}\right]_{\min} \simeq (1+X)^{-1}[1-\Omega_2/n + X^4(1-\Omega_1/n)]^{1/4} ; \qquad (2.25)$$

in other words, when the post-Newtonian approximation breaks down.

In summary, for coalescing binaries containing one or more neutron stars, we shall terminate our purely gravitational orbital evolution at separations between 10 and $7m$, when tidal stripping is expected to dominate, and for black holes, we shall terminate the evolution around $2m$, when the entire approximation breaks down.

III. EVOLUTION OF THE ORBIT

A. Evolution of nonrelativistic systems

When the parameter $m/p \ll 1$, so that the relativistic corrections in the Lagrange planetary equations are small, and so that the time scale for gravitational-radiation damping is much longer than an orbital time scale, Eqs. (2.11) can be solved by iteration: substitute initial, constant values for e, ω, p, etc., into the right-hand sides, and integrate. When integrated over a complete orbit ($\Delta\phi = 2\pi$) the results are

$$\Delta e = -(\eta e/15)(m/p)^{5/2}(304+121e^2) , \qquad (3.1a)$$

$$\Delta(p/m) = -(8\eta/5)(m/p)^{3/2}(8+7e^2) , \qquad (3.1b)$$

$$\Delta\omega = 6\pi m/p + O((m/p)^2) . \qquad (3.1c)$$

For e and p, the post- and post-post Newtonian effects are small and purely periodic; only the radiation reaction terms have a secular effect, while for ω, the post-Newtonian term contributes at leading order, giving the well-known relativistic periastron advance. Taking the ratio of Eqs. (3.1a) and (3.1b), we obtain an equation for the "orbit averaged" derivative de/dp, which can be integrated to yield[31]

$$\frac{p}{p_i} = \left[\frac{e}{e_i}\right]^{12/19}\left[\frac{304+121e^2}{304+121e_i^2}\right]^{870/2299} . \qquad (3.2)$$

A multiple-scale analysis of the Lagrange planetary equations yields the same result (Appendix A). From Eq. (3.1b), the orbit-averaged p necessarily decreases with time. Thus as the orbit shrinks because of gravitational-radiation losses, the average e decreases, consequently the orbit is "circularized" by gravitational-radiation damping. This is expected because gravitational radiation decreases both the energy and the angular momentum of the orbit.

B. Relativistic systems and quasicircular orbits

According to Eq. (3.2), e decreases, while m/p increases. Eventually, the leading relativistic perturbation on the right-hand side of Eq. (2.11a), of order m/p, will be comparable to e itself. The question is, what is the subsequent evolution of the system in the language of osculating elements, and does it correspond to a circular orbit? A true circular orbit cannot be a solution to our (post)$^{5/2}$-Newtonian equations, of course, since the radiation-reaction terms cause an inspiral of the system. Instead, one might ask whether it is possible to find a solution to the post-post-Newtonian order equations (i.e., without radiation-reaction terms) which is a circular orbit. The obvious guess of seeking a solution for which $e=0$ fails immediately since, according to Eq. (2.11a), $de/d\phi \neq 0$ when $e=0$.

On the other hand, from Eq. (2.11b), as e becomes comparable to m/p, $d\omega/d\phi$ becomes comparable to unity, in other words, the periastron advances at a rate comparable to the orbital motion. This suggests that we try an elliptical osculating orbital of fixed p and nonzero e which precesses at the *same* rate as the orbital motion. This will produce an actual orbit which is circular, since the particle will always be at the same point on the osculating ellipse as they both revolve. The condition that the particle and osculating orbit advance at the same rate means that $d\omega/d\phi = 1$ or that $f=\phi-\omega$ is a constant. A solution will exist if we can choose a value of f so that the Lagrange planetary equations reduce to a consistent set of equations. Trying $f=\pi$, in Eqs. (2.11a) and (2.11c), we have, to post-post-Newtonian order,

$$de/d\phi = 0, \quad dp/d\phi = 0 , \qquad (3.3)$$

and, since $e\, d\omega/d\phi \equiv e$, we obtain, from Eq. (2.11b) or (2.9c),

$$e = A_1 + A_2 . \qquad (3.4)$$

Solving Eq. (3.4) iteratively we see that these equations will be consistent if

$$e \approx (3-\eta)m/p - (15+\tfrac{17}{4}\eta+2\eta^2)(m/p)^2 . \qquad (3.5)$$

Substituting these orbital elements into the definitions of the orbit, Eqs. (2.8), we obtain

$$r=p/(1-e)$$
$$\approx p[1+(3-\eta)m/p-(6+\tfrac{41}{4}\eta+\eta^2)(m/p)^2]\ , \qquad (3.6a)$$
$$v\approx(m/p)^{1/2}[1-(3-\eta)m/p+(15+\tfrac{17}{4}\eta+2\eta^2)(m/p)^2]$$
$$\times(-\mathbf{e}_x\sin\phi+\mathbf{e}_y\cos\phi)\ , \qquad (3.6b)$$
$$\phi=nt+\phi_0\ , \qquad (3.6c)$$
$$n\approx(m/p^3)^{1/2}[1-2(3-\eta)m/p$$
$$+(39+\tfrac{5}{2}\eta+5\eta^2)(m/p)^2]\ , \qquad (3.6d)$$

which are equivalent through post-Newtonian order to the circular orbit formulas of Wagoner and Will.[19]

The radiation-reaction terms in the full (post)$^{5/2}$-Newtonian equations will produce a secular decrease in e and p, in addition to periodic variations, thus preventing the static circular solution found above. However, since the (post)$^{5/2}$-Newtonian terms are a perturbation on the post-post-Newtonian equations, one might seek a "quasicircular" solution of the form

$$e\approx(3-\eta)u-(15+\tfrac{17}{4}\eta+2\eta^2)u^2+\delta e\ u^q,\quad q\geq 5/2\ , \qquad (3.7a)$$
$$f\approx\pi+f_1u^r,\quad r\geq 1\ , \qquad (3.7b)$$

where $u\equiv m/p$. Substituting this ansatz into the Lagrange planetary equations we have

$$de/d\phi\simeq-(3-\eta)u^{r+1}f_1+\tfrac{64}{5}\eta u^{5/2}+O(u^{r+2})\ , \qquad (3.8a)$$
$$du/d\phi=-u^2d(p/m)/d\phi$$
$$\simeq u^2[\tfrac{64}{5}\eta u^{3/2}+4(2-\eta)(3-\eta)u^{r+1}f_1$$
$$-\tfrac{144}{5}\eta(3-\eta)u^{5/2}+O(u^{r+2})]\ , \qquad (3.8b)$$

and thus

$$\frac{de}{du}\simeq\frac{\tfrac{64}{5}\eta u^{3/2}-(3-\eta)u^rf_1+O(u^{r+1})}{u[\tfrac{64}{5}\eta u^{3/2}+4(2-\eta)(3-\eta)u^{r+1}f_1-\tfrac{144}{5}\eta(3-\eta)u^{5/2}+O(u^{r+2})]}\ . \qquad (3.9)$$

However, this equation must be consistent with the original ansatz, which gives $de/du\approx(3-\eta)+O(u)$. This yields a solution for f_1 provided $r=3/2$. The result is

$$f\approx\pi+\frac{64}{5}\frac{\eta}{3-\eta}u^{3/2}+O(u^{5/2})\ . \qquad (3.10)$$

Substituting this and Eq. (3.7a) back into Eq. (2.11b), we find that $q=3$, so that the original solution for e [Eq. (3.5)] is valid through (post)$^{5/2}$-Newtonian order. With this solution we then find that u and ϕ evolve according to

$$du/d\phi\approx(64/5)\eta u^{7/2}+O(u^{9/2})\ , \qquad (3.11a)$$
$$d\phi/dt\equiv(mp)^{1/2}r^{-2}\approx m^{-1}u^{3/2}+O(u^{5/2})\ , \qquad (3.11b)$$

with the solutions

$$p=p_i[1-(256/5)\eta u_i^4(t-t_i)/m]^{1/4}\ , \qquad (3.12a)$$
$$\phi=\phi_i+(32\eta u_i^{5/2})^{-1}$$
$$\times\{1-[1-(256/5)\eta u_i^4(t-t_i)/m]^{5/8}\}\ . \qquad (3.12b)$$

The orbit can then be obtained from Eqs. (3.6a) and (3.6b). Notice that the number of orbits and the elapsed time to coalescence from an initial value of p are given approximately by

$$\Delta t\approx(5m/256\eta)(p_i/m)^4$$
$$\approx(0.42s)(4\eta)^{-1}(m/2.8\ M_\odot)(p_i/25m)^4\ , \qquad (3.13a)$$
$$N\approx(64\pi\eta)^{-1}(p_i/m)^{5/2}$$
$$\approx 62(4\eta)^{-1}(p_i/25m)^{5/2}\ . \qquad (3.13b)$$

Is this quasicircular orbit an isolated solution of the Lagrange planetary equations, or is it the end point of evolution of a general initially nonrelativistic orbit? In an appendix we verify that it is the latter. Using a "two-scale analysis" of the planetary equations, we find that the orbit averaged e^2 evolves according to

$$\langle e^2\rangle\approx e_i^2(u_i/u_0)^{19/6}+(3-\eta)^2u_0^2\ , \qquad (3.14)$$

where u_0 represents the leading, secular behavior of m/p, given by Eq. (3.12a), u_i is its initial value, and e_i is the initial eccentricity. Initially, $u_0=u_i\ll e_i$, and thus the initial term dominates, leading to the behavior described in Sec. III A, Eq. (3.2). As u_0 increases, the first term decreases, while the second increases, and eventually the quasicircular behavior of the eccentricity of Eq. (3.5) is established. Figure 6 shows the behavior of e as a function of u_0, for various initial values of u and e. Systems will evolve toward the right down an approximately straight line with slope $-19/12$ until they reach the line marked "quasicircular orbits" whereupon they evolve up to the right. The different tracks correspond to different initial values of e for a given initial u. If the orbits are projected backwards in time, and if their evolution is governed purely by the post-Newtonian equations with radiation reaction, it is known that they necessarily become unbound ($e\geq 1$) at a finite value of p, and at a finite time in the past.[32]

Whether or not an orbit has time to circularize, say, before tidal forces becomes dominant, or before the post-Newtonian scheme breaks down at $u_0\approx 1$ can be determined from the figure. For example, a system such as the binary pulsar (track labeled A), with $e_i\approx 0.6$ and $u_i\approx 3\times 10^{-6}$, will circularize when $u\approx 10^{-4}$, well before tidal effects are significant. On the other hand, a double neutron-star system formed by capture due to gravitational-radiation dissipation in a dense cluster of

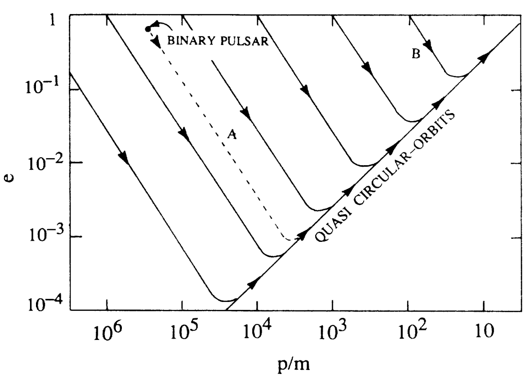

FIG. 6. Evolution of osculating eccentricity as a function of p/m. Gravitational-radiation damping causes p to decrease, so systems evolve from left to right. For systems with $e \gg m/p$ eccentricity decreases approximately as $(p/p_i)^{19/12}$, until quasicircular condition $e \approx (3-\eta)m/p$ is reached. Current state of binary pulsar PSR 1913+16 is marked; its future evolution will follow track A. Track B denotes evolution of system captured into a highly eccentric, bound orbit, with $p_i/m \approx 100$; such a system barely becomes quasicircular before relativistic plunge occurs (cf. Fig. 12).

compact stars, with an initial periastron separation of around 200 km (Ref. 7b) (track B), would have $e_i = 1$ with $u_i \approx 10^{-2}$ and would be likely to remain elliptical until tidal or hydrodynamical effects set in. The analogous capture of two black holes will not approach a quasicircular orbit until $u \approx 0.1$, at which point the orbit enters a final "plunge" phase. These qualitative considerations are confirmed by the numerical solutions discussed in the next subsection.

C. Numerical evolution of orbits

The approximate analytic solutions obtained in the previous subsection relied upon the assumption that $m/p \ll 1$. In the late stage of coalescence, this assumption is no longer valid, and a direct numerical integration of the Lagrange planetary equations is needed to follow the evolution further, until the entire $(\text{post})^{5/2}$-Newtonian approximation breaks down. The results of such numerical integrations serve two purposes, first to provide input for the gravitational wave forms summarized in Sec. II C, and second to provide approximate initial conditions for further evolution of such systems using hydrodynamic or fully general-relativistic codes.[13]

We begin with the quasicircular case. This case gives a single, universal orbit for each value of $\eta = \mu/m$, for the following reason. Since both ω and e are functions of m/p, the solution depends only on the initial value of p. Since p decreases secularly with time, then for any p/m, the solution depends only on the initial moment of time, which is arbitrary. The only factor which distinguishes one quasicircular orbit from another is the orientation in space, which is determined by the fixed inclination i and angle of nodes Ω, and by the time of initial periastron passage. This universality is also illustrated by the common quasicircular track in Fig. 6.

Consider a system of equal masses ($\eta = 1/4$). Working

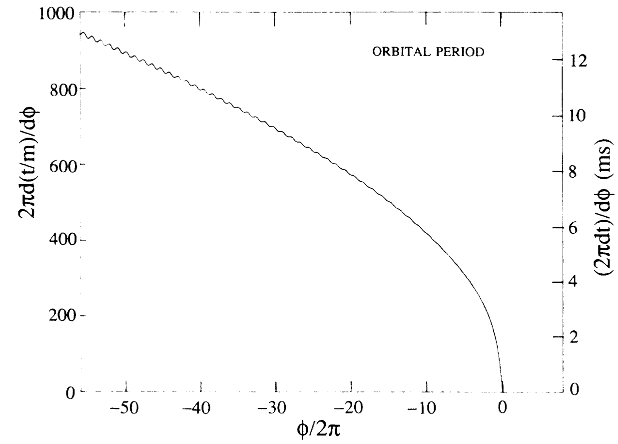

FIG. 7. Evolution of "orbital period," $2\pi d(t/m)/d\phi$ for equal-mass quasicircular orbit. Scale at right gives period in milliseconds for two 1.4 $M_\odot$ bodies.

in terms of the rescaled time t/m, and beginning the numerical integration at $p_i/m = 25$, we find the solutions summarized in Figs. 1, 2, 7, and 8. The initial values of e and ω are determined from Eqs. (3.7a) and (3.10). Figure 1 shows e, p/m, and the orbital separation r/m as functions of ϕ. The initial residual oscillations are a consequence of the fact that the chosen initial conditions are still only an approximation to the true quasicircular orbit. As the orbit evolves, these oscillations damp out as the orbit becomes more quasicircular; r/m decreases, while $e \approx 2.75m/p$ increases. Figure 2 shows the actual relative orbit in space; the points marked 10, 7, 5, and 2, correspond to values of r/m. The final "plunge" orbit begins around $r = 7m$. Figure 7 shows the evolution of $2\pi d(t/m)/d\phi$, which is a rough measure of the instantaneous orbital period in units of m. Notice that, for a system of two $1.4M_\odot$ bodies, the period decreases from about 13 ms when $r \approx 25m$ to about 3 ms when $r \approx 10m$ in an interval of about 0.5 s. Figure 8 gives the radial and tangential velocities as a function of the separation r. Ini-

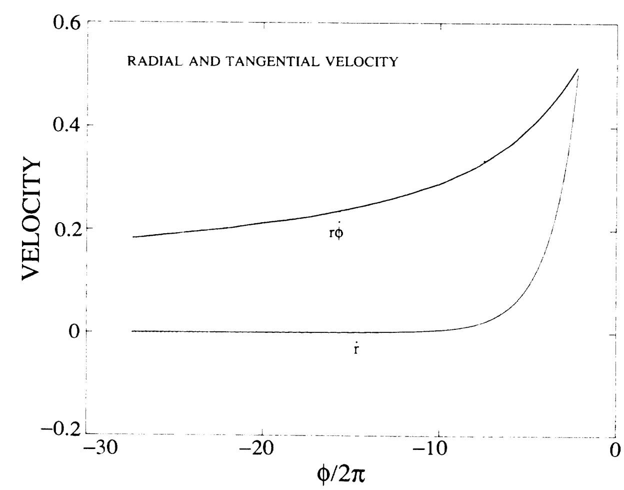

FIG. 8. Radial and tangential orbital velocities for equal-mass quasicircular orbit.

tially, the radial velocity is very small because the orbit is a slowly decaying circle, but by the time of the plunge, the radial and tangential velocities are comparable. These velocity values could be used as initial conditions for a given initial separation to begin a hydrodynamical evolution of two coalescing neutron stars.[13]

Notice that the orbit decays from $p=25m$ in about 55 orbits, about 10% fewer than the estimate given in Eq. (3.13b). The latter estimate was obtained from Eqs. (3.11), which procedure amounts to inserting the Newtonian approximation for the orbit into the radiation-reaction terms. However, in the numerical solution, the full (post)$^{5/2}$-Newtonian orbit is inserted into all terms at each stage of the evolution. Formally, this is inconsistent, since the (post)$^{5/2}$-terms $A_{5/2}$ and $B_{5/2}$ in Eqs. (2.4) have already been simplified using Newtonian equations of motion, and the higher-order, (post)$^{7/2}$-Newtonian terms have been neglected. Thus the secular evolution of the orbital separation is accurate up to a relative error of order m/p, which in this example is around 10%. Therefore, this analysis cannot reliably determine whether the actual orbit will decay more quickly or more slowly than the Newtonian estimate (3.13b); only a fully general-relativistic analysis can do so.

For stars with a mass ratio of 10:1 ($\eta=10/121$), the orbits are shown in Figs. 9 and 10. Since the quasicircular values of e and ω are only weakly dependent on η, the dominant change is in the time scale for decay of the orbit, which is inversely proportional to η. Figure 9 shows the expected threefold increase in the number of orbits for decay. From Fig. 10, we see a slower spiral and a final plunge which occurs at a much smaller separation, around $4m$. In fact, further decrease of η would lead to

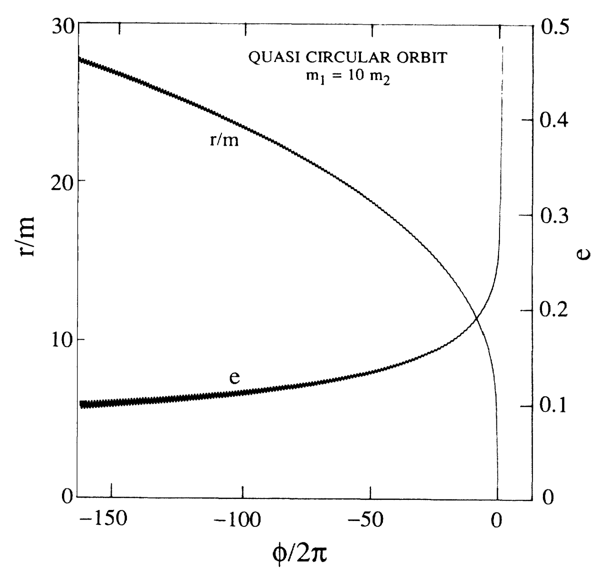

FIG. 9. Evolution of e and r/m for $m_1=10m_2$ quasicircular orbit, plotted against $\phi/2\pi\approx$number of orbits. Initial condition is $p_i=25m$. Approximately three times as many orbits are required to coalesce compared to equal-mass case (Fig. 1) because gravitational-radiation damping (proportional to $\eta=\mu/m$) is three times weaker.

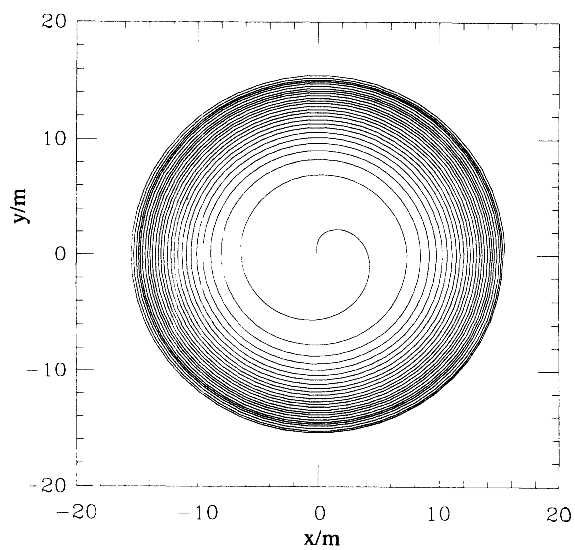

FIG. 10. Quasicircular relative orbit for $m_1=10m_2$.

quasicircular motion without a plunge persisting to smaller and smaller separations: even though $m/p\rightarrow 1$ and the post-Newtonian corrections are becoming large, the radiation-damping term remains small because of the smallness of η. Very small values of η would correspond astrophysically to a stellar-mass neutron star or black hole spiraling into a supermassive black hole. However, in such cases the post-Newtonian approximation used here is inadequate to approximate the final motion, because it does not properly describe the existence of an innermost circular orbit for test-body motion around a black hole, which occurs at $r=5m$ for a nonrotating hole (in harmonic coordinates), inside which the body would plunge toward the hole, even with arbitrarily weak radiation damping. For two comparable-mass holes, such an innermost orbit also exists,[4] but as Fig. 2 shows, gravitational-radiation damping in that case is sufficiently strong to produce a plunge before that orbit is reached.

Another set of orbital solutions is shown in Figs. 11–13, corresponding to equal masses, with the initial condition $e=1$. These highly noncircular orbits would be produced by binary capture due to gravitational-radiation damping in a dense cluster of compact stars. Quinlan and Shapiro[7b] argued that this process plays an important role in the evolution of such clusters, and could lead to promising sources of gravitational waves. They showed that the maximum value of p/m leading to such capture is given by

$$\left[\frac{p}{m}\right]_{\max}\approx 90(4\eta)^{2/7}\left[\frac{|v_1-v_2|}{10^3\ \mathrm{km\,s^{-1}}}\right]^{-4/7}. \tag{3.15}$$

For initial values of p we choose 90 and $40m$. Figure 11 shows the evolution of the eccentricity in the two cases. The results confirm the behavior discussed in Sec. III C: decrease of the average eccentricity (while oscillating because of periodic post-Newtonian corrections) until $e\approx m/p$, then an increase, together with a reduction in the amplitude of oscillations as the orbit approaches the quasicircular state of Eq. (3.5), and then a rapid increase as the plunge ensues. Notice that in neither case does the orbit quite make it to the quasicircular state. This is also shown in Fig. 12 which displays the evolution of the orbital separation in the final 20 orbits in each case. The noncircular nature of these orbits will be reflected in the gravitational wave forms (Sec. IV). The orbit in space of the more compact capture ($p = 40m$) is shown in Fig. 13; the rapid advance of the periastron as the orbit decays and attempts to circularize is apparent.

IV. GRAVITATIONAL WAVE FORMS AND LUMINOSITY

The analytic and numerical solutions for the orbits obtained in the previous section yield the coordinate relative position vector $\mathbf{x}(t)$ and velocity $\mathbf{v}(t)$ as functions of time, through (post)$^{5/2}$-Newtonian order. These are then input for the post-Newtonian gravitational wave forms of Sec. II C, Eqs. (2.12) and (2.13).

For the quasicircular case, the wave forms can be written to post-Newtonian order in a relatively simple form using the solutions of Eqs. (3.6), with the result

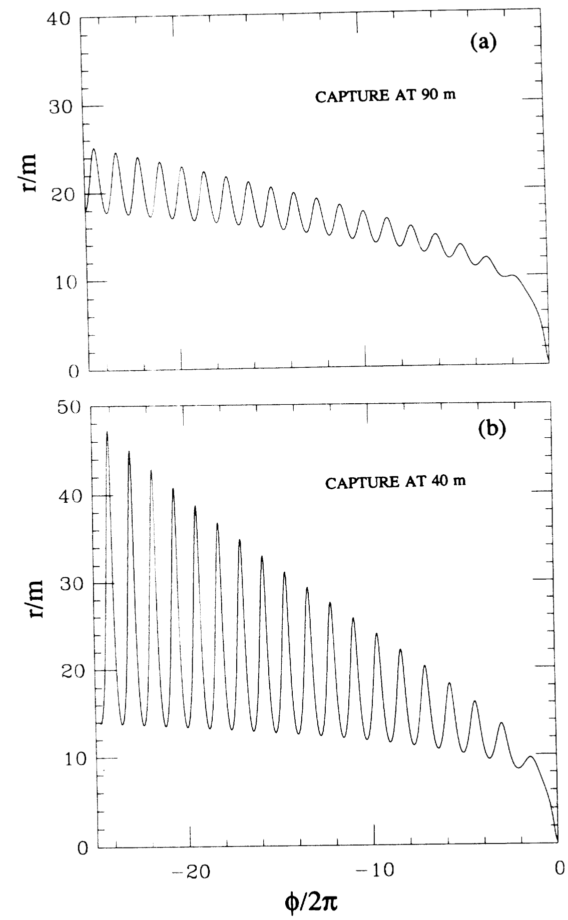

FIG. 12. Evolution of separation for equal-mass capture orbits. Final 25 revolutions are shown in each case.

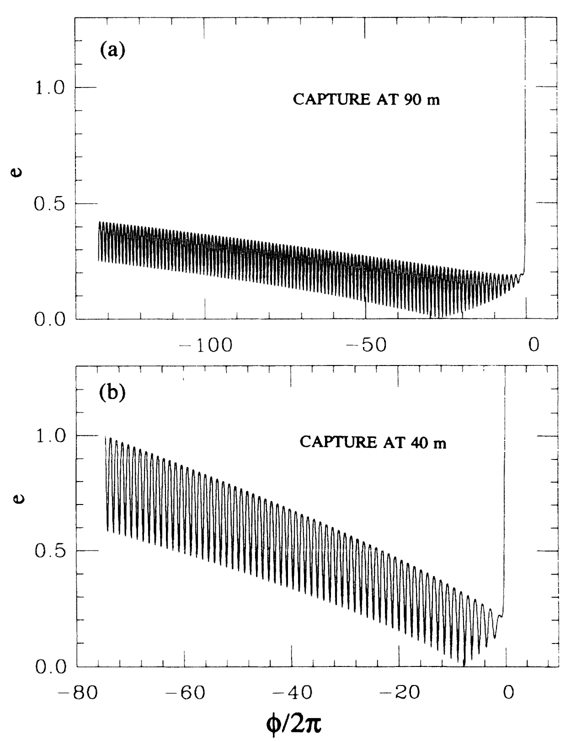

FIG. 11. Evolution of eccentricity for equal-mass capture orbits with initial p_i of (a) $90m$ and (b) $40m$. Initially, eccentricity decreases on average, while oscillating because of post-Newtonian perturbations; as quasicircular state is approached, average eccentricity increases while amplitude of oscillations decreases. Neither system quite reaches true circularity before plunge.

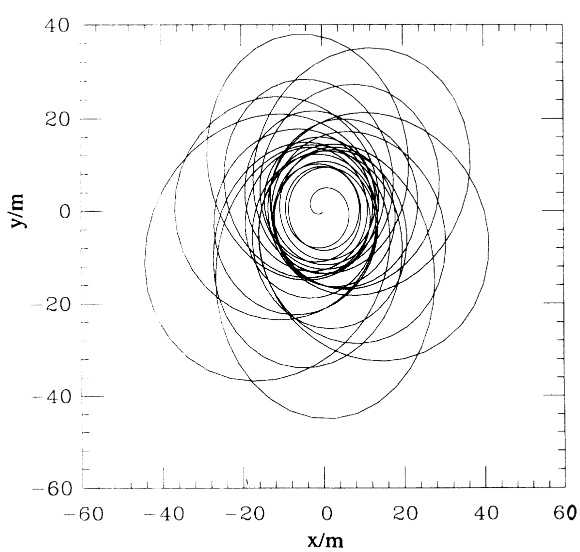

FIG. 13. Relative orbit for equal-mass capture at $40m$, showing final 20 revolutions. Rapid advance of apastron is evident.

$$h_+ \approx -\frac{2\mu}{R}\left[\left[\frac{m}{p}\right](1+\cos^2\Theta)\cos2\Psi - \frac{1}{2}\left[\frac{m}{p}\right]^{3/2}\frac{\delta m}{m}\sin\Theta[\sin\Psi+\tfrac{1}{4}(1+\cos^2\Theta)(\sin\Psi+9\sin3\Psi)]\right.$$
$$\left. -\frac{1}{3}\left[\frac{m}{p}\right]^2\{\tfrac{1}{2}(37-9\eta)(1+\cos^2\Theta)\cos2\Psi+(1-3\eta)\sin^2\Theta[2\cos2\Psi+(1+\cos^2\Theta)(\cos2\Psi+4\cos4\Psi)]\}\right], \tag{4.1a}$$

$$h_\times \approx \frac{2\mu}{R}\cos\Theta\left[2\left[\frac{m}{p}\right]\sin2\Psi+\frac{3}{4}\left[\frac{m}{p}\right]^{3/2}\frac{\delta m}{m}\sin\Theta(\cos\Psi+3\cos3\Psi)\right.$$
$$\left. -\frac{1}{3}\left[\frac{m}{p}\right]^2[(37-9\eta)\sin2\Psi+4(1-3\eta)\sin^2\Theta(\sin2\Psi+2\sin4\Psi)]\right], \tag{4.1b}$$

where $\Psi \equiv \Phi - \phi$, and where p and ϕ evolve according to Eqs. (3.12). However, in the following numerical results, the full orbital solution was substituted into the original wave forms (2.13). For the equal-mass quasicircular case, Fig. 14 shows the wave forms $(R/2\mu)h_+$ and $(R/2\mu)h_\times$ for various observing angles relative to the orbit, plotted as functions of ϕ. Shown are the waves from the final eight orbits before termination of the evolution at $r \approx 5m$. Because of the equal-mass symmetry, the waves occur predominantly at twice the orbital frequency. The amplitude increases with time roughly as m/p. For neutron-star binaries, the wave form generated by purely gravita-

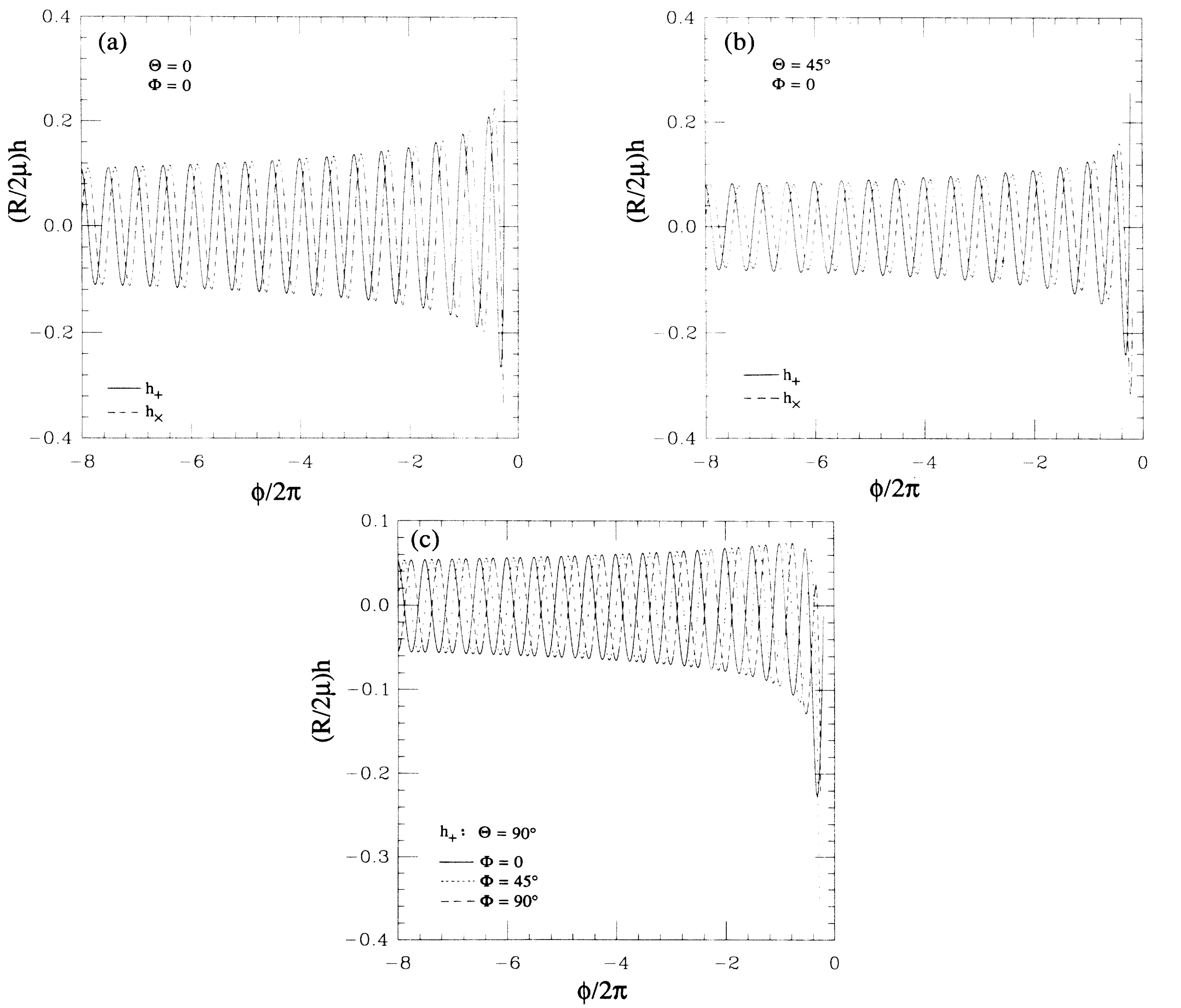

FIG. 14. Gravitational wave forms h_+ and $h_\times$ for equal-mass quasicircular orbit. Shown are observation directions along orbital axis, 45° from the axis, and in the orbital plane (where $h_\times \equiv 0$).

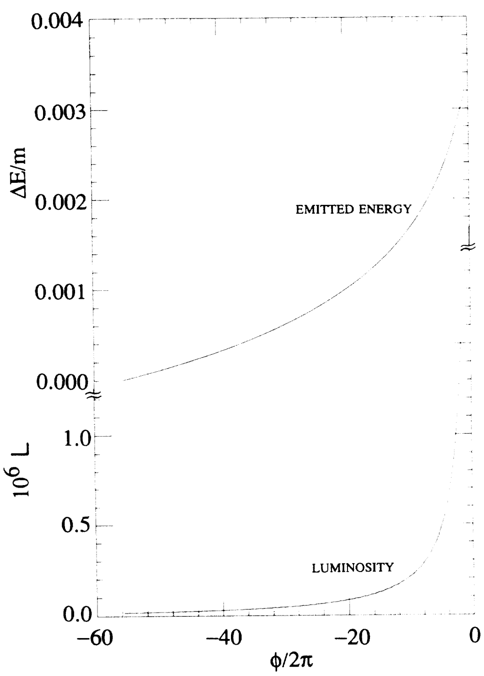

FIG. 15. Gravitational luminosity and emitted energy for equal-mass quasicircular orbit.

tional motion would be cut off around $r=7-10m$, corresponding to $\phi/2\pi\simeq-1$ to -2. The post-Newtonian corrections in the wave forms increase from around 7% of the total wave form at $p\approx25m$ to almost 10% at termination. If we denote the amplitudes plotted in Fig. 14 by $\tilde{h}$, then the observed wave forms at Earth will have the amplitude

$$h_{\rm obs}\approx7\times10^{-23}(4\eta)\left[\frac{m}{2.8M_\odot}\right]\left[\frac{100\ {\rm Mpc}}{R}\right]\left[\frac{\tilde{h}}{0.1}\right]. \tag{4.2}$$

The gravitational luminosity and the integrated emitted energy are plotted in Fig. 15. The dimensionless luminosity 10^{-6} corresponds to 3.6×10^{53} erg s^{-1} or 0.2 $M_\odot$s^{-1}. The numerical results for the luminosity are cut off somewhat earlier than those for the orbit and wave form because the post-Newtonian correction in Eq. (2.15), which turns out to be negative, becomes comparable to the Newtonian term early because of large numerical coefficients, causing the total luminosity eventually to turn negative. An "exact" expression for the luminosity must, of course, be positive definite; thus, in some sense, our result can be viewed as a lower limit on the luminosity. This problem illustrates the inherent danger in pushing approximations to the limit of their validity. Wagoner and Will[19] offer alternative expressions for the post-Newtonian luminosity for circular orbits in an attempt to mitigate this problem; however, in the absence of higher-order terms, there is no unique way to do this.

For unequal masses, in the ratio 10:1, the wave forms for the final seven orbits are shown in Fig. 16. The h_+ wave forms in the orbital plane [Fig. 16(b)] show additional components at the orbital frequency and at three times the orbital frequency, because of the mass asymmetry [cf. $\delta m/m$ terms in Eq. (4.1)]. The dependence on Φ of these orbital-plane wave forms, primarily in the final orbit, reflects asymmetric beaming of the radiation, which could lead to a net radiation of momentum and a consequent recoil of the system.[9b] We are currently addressing this question.

The capture orbits lead to a complex wave form and luminosity, shown in Figs. 17 and 18 for the case of capture at $p=40m$. Shown are the final 24 or so orbits, by which point the eccentricity has decreased to 0.2, and the minimum separation at periastron is around $14m$. The wave form here is plotted against time. The sharp pulses correspond to radiation emitted at periastron. The changing shape of both the pulses and of the interpulse waveforms reflects the rapid advance of the periastron relative to the line of sight, as seen in Fig. 13. The wave form from the final few orbits in each case is shown on an expanded scale, illustrating the trend toward a circular orbit in the final stage of coalescence.

V. CONCLUDING REMARKS

We have used an approximation procedure to study in detail the coalescence of a binary system of compact objects. In the final analysis, a complete description of this process will require the full machinery of general-relativistic hydrodynamics or of black-hole interactions, carried out in a complete numerical integration of Einstein's equations. Nevertheless, the post-Newtonian approximation which we have employed gives accurate results in appropriate cases. The orbital evolution is formally accurate up to errors of $O((m/p)^3)$ in the instantaneous orbit and up to relative errors of $O(m/p)$ in the secular decay of the orbit, while the wave forms are formally accurate up to errors $O((m/p)^2)$ relative to the dominant contribution. For neutron-star systems, we terminate the evolution around $p\approx10m$ because of the dominance of tidal effects, thus we expect the orbit to be accurate to a tenth of a percent instantaneously, and the wave form to be accurate to 1%. For two-black-hole systems, we continue the evolution to $p\approx2m$, by which point the approximations have become invalid.

To improve the accuracy of these results further would require extending both the equations of motion and the gravitational wave forms to higher post-Newtonian order. It remains to be seen whether the benefits of such extensions would outweight the effort, in view of the progress being made in the realm of numerical relativity.

However, one simple extension may yield a payoff. The axial asymmetry that appeared in the wave forms for the unequal-mass quasicircular case [Fig. 16(b)] suggests an asymmetry in the radiated energy, and thereby a possible recoil of the system. The net momentum radiated by a coalescing binary system depends on a cross term between the "half-order" or $\delta m/m$ terms in the gravitational wave form h^{ij}, and the dominant Newtonian quadrupole term. If the quadrupole term is $O(m/p)$, this term is $O((m/p)^{3/2})$. Therefore, by determining the $O((m/p)^{5/2})$ term in the wave form, we can obtain a more accurate expression for the momentum radiated. This term has already been calculated formally by Epstein and Wagoner,[23] and should be readily reducible to the binary-system form. Using our accurate orbital evolution we will then be able to obtain an improved estimate for the gravitational radiation "rocket effect" for two black holes, and can then study its astrophysical implications.[9(b)]

Another possible extension of our approach which will be important for neutron-star coalescence, is the incorporation of tidal effects, possibly by the *ad hoc* device of adding a Newtonian-style tidal potential to the equations of motion.

These and other applications of the methods developed in this paper are currently under study.

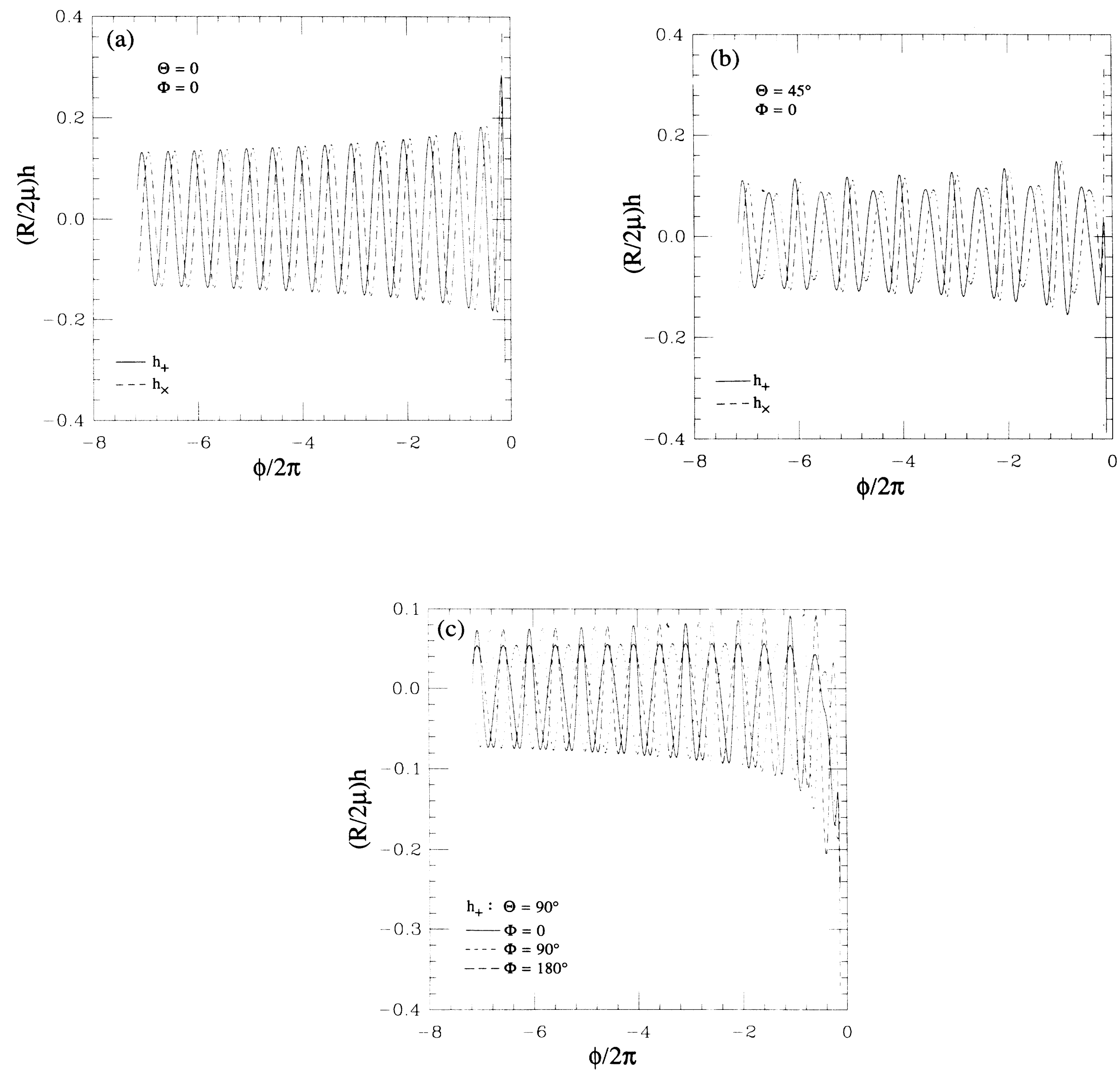

FIG. 16. Gravitational wave forms h_+ and $h_\times$ for $m_1 = 10m_2$ quasicircular orbit. Observation directions are as in Fig. 14. For directions other than orbital axis, mass asymmetry introduces waves at one and three times orbital frequency, in addition to those at twice and four times orbital frequency, leading to modulation shown. Wave-form asymmetry in orbital plane (c) during final plunge may represent net radiation of momentum, leading to recoil of system.

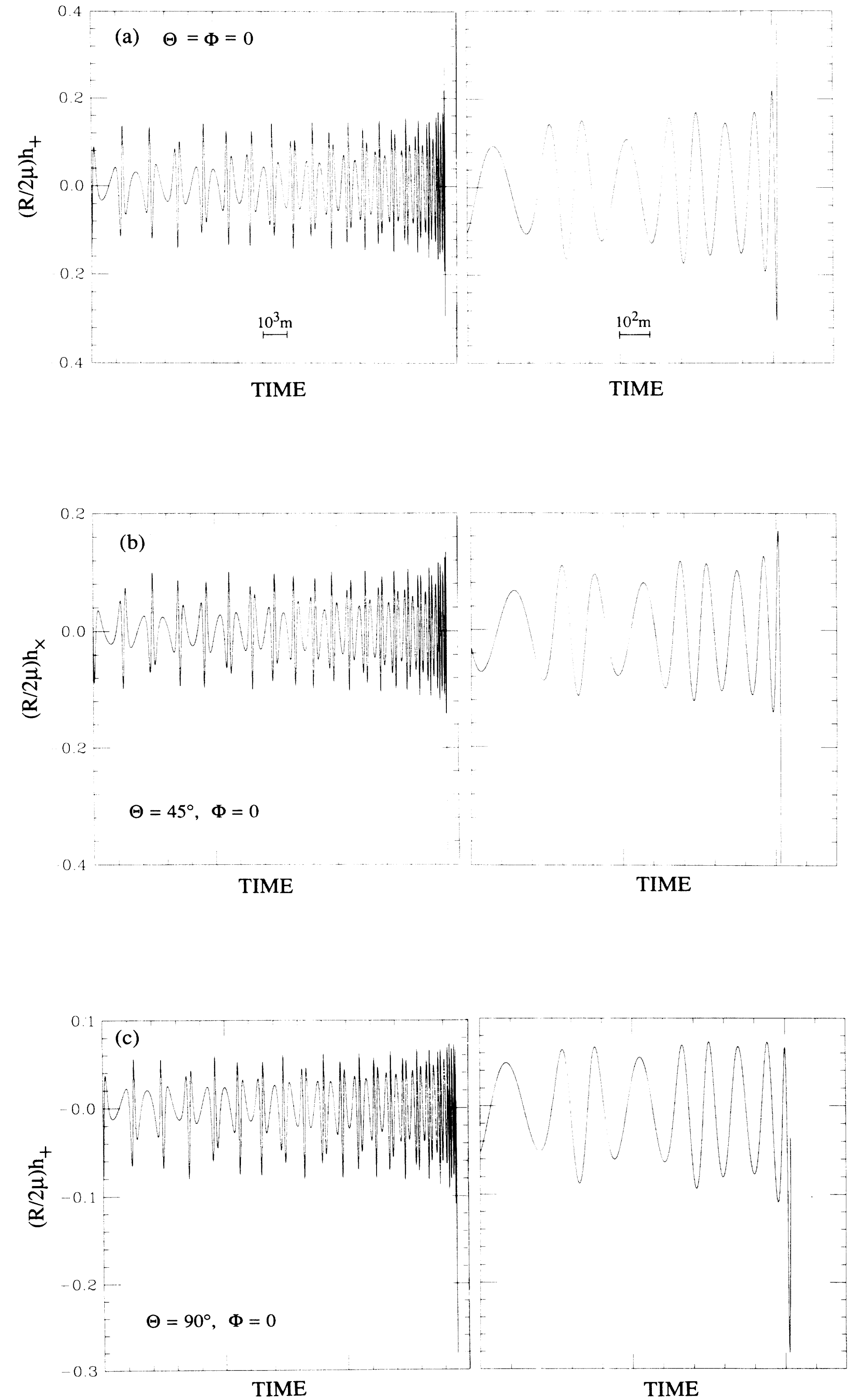

FIG. 17. Gravitational wave forms for equal-mass capture orbit at $40m$. Right-hand panel shows final wave form on a time scale expanded by factor of 10. Sharp bursts are emitted at periastron; evolving interburst wave-form shape reflects rapid advance of periastron (Fig. 13) relative to line of sight.

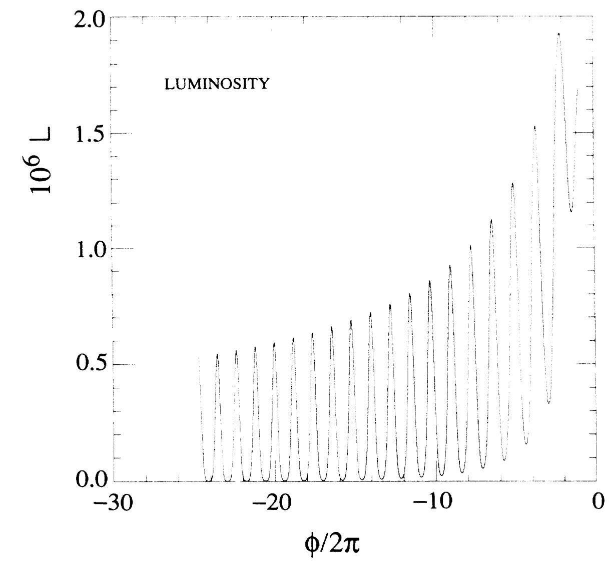

FIG. 18. Gravitational luminosity for equal-mass capture orbit at $40m$.

ACKNOWLEDGMENTS

This research was supported in part by the National Science Foundation Grants Nos. PHY 85-13953 and PHY 89-22140.

APPENDIX A: EVOLUTION OF ORBITS TO THE QUASICIRCULAR STATE

In Sec. II B we found a quasicircular solution of the Lagrange planetary equations given by the orbit elements

$$e \approx (3-\eta)u - (15+\tfrac{17}{4}\eta+2\eta^2)u^2 + O(u^3) ,$$
$$f \approx \pi + \tfrac{64}{5}\eta(3-\eta)^{-1}u^{3/2} + O(u^{5/2}) , \qquad \text{(A1)}$$

where $u = m/p$, and where u evolves according to

$$u \approx u_i[1-\tfrac{256}{5}\eta u_i^4(t-t_i)/m]^{-1/4} . \qquad \text{(A2)}$$

Here we demonstrate that this is the general late-time evolution of a binary system governed by the $(\text{post})^{5/2}$-Newtonian equations of motion, given sufficient radiation-reaction damping before the approximation breaks down. (Because the approximation becomes worse as the desired evolution proceeds, this analysis will not be rigorous. This is to be contrasted with the rigorous analysis by Walker and Will[32] of the evolution projected toward the infinite past, where the post-Newtonian approximation becomes better and better.)

Because the initial, nonrelativistic evolution given by Eq. (3.1) leads to small values of e, we use the nonsingular planetary equations for α and β, instead of those for e and ω, Eqs. (2.11). These have the form

$$\begin{aligned}
d\alpha/d\phi = {} & (m/p)\{(3-\eta)\sin\phi - 3\beta + (5-4\eta)(\alpha\sin2\phi-\beta\cos2\phi) \\
& + \tfrac{1}{8}[(56-47\eta)\alpha^2-(8+21\eta)\beta^2]\sin\phi - \tfrac{1}{4}(32-13\eta)\alpha\beta\cos\phi + \tfrac{3}{8}\eta(\beta^2-\alpha^2)\sin3\phi + \tfrac{3}{4}\eta\alpha\beta\cos3\phi\} \\
& + (m/p)^2\{-\tfrac{1}{4}(36+73\eta-8\eta^2)\sin\phi - (7+5\eta-7\eta^2)\beta + (11+31\eta-3\eta^2)(\beta\cos2\phi-\alpha\sin2\phi) \\
& - \tfrac{1}{16}[(92+181\eta-32\eta^2)\alpha^2+(84+79\eta-224\eta^2)\beta^2]\sin\phi + \tfrac{1}{8}(4+51\eta+96\eta^2)\alpha\beta\cos\phi \\
& + \tfrac{1}{16}(60+245\eta-64\eta^2)[(\beta^2-\alpha^2)\sin3\phi+2\alpha\beta\cos3\phi] + \tfrac{1}{8}(2-21\eta+48\eta^2)\beta(\alpha^2+\beta^2) \\
& - \tfrac{1}{2}[(3-11\eta-10\eta^2)\alpha^2-(3-10\eta+14\eta^2)\beta^2]\alpha\sin2\phi \\
& + \tfrac{1}{4}[(12-43\eta-16\eta^2)\alpha^2-(\eta+24\eta^2)\beta^2]\beta\cos2\phi \\
& - \tfrac{1}{8}(2+25\eta-16\eta^2)[(\alpha^2-3\beta^2)\alpha\sin4\phi-(3\alpha^2-\beta^2)\beta\cos4\phi] \\
& + \tfrac{1}{64}\eta[(477+161\eta)\alpha^4+6(57+61\eta)\alpha^2\beta^2-5(27-41\eta)\beta^4]\sin\phi \\
& - \tfrac{1}{16}\eta(153-11\eta)\alpha\beta(\alpha^2+\beta^2)\cos\phi + \tfrac{3}{128}\eta[(73+53\eta)\alpha^4-6(53+17\eta)\alpha^2\beta^2+(33-19\eta)\beta^4]\sin3\phi \\
& - \tfrac{3}{32}\eta[7(9+5\eta)\alpha^2-(43-\eta)\beta^2]\alpha\beta\cos3\phi \\
& - \tfrac{15}{128}\eta(1-3\eta)[(\alpha^4-6\alpha^2\beta^2+\beta^4)\sin5\phi-4(\alpha^2-\beta^2)\alpha\beta\cos5\phi]\} \\
& - \tfrac{1}{15}\eta(m/p)^{5/2}\{192\cos\phi+304\alpha+320(\alpha\cos2\phi+\beta\sin2\phi)+(538\alpha^2+230\beta^2)\cos\phi+308\alpha\beta\sin\phi \\
& + 182(\alpha^2-\beta^2)\cos3\phi+364\alpha\beta\sin3\phi+121\alpha(\alpha^2+\beta^2)+10(23\alpha^2+13\beta^2)\beta\sin2\phi \\
& + 20(9\alpha^2+4\beta^2)\alpha\cos2\phi+35(\alpha^2-3\beta^2)\alpha\cos4\phi+35(3\alpha^2-\beta^2)\beta\sin4\phi \\
& + 6(5\alpha^4+8\alpha^2\beta^2+3\beta^4)\cos\phi+12(\alpha^2+\beta^2)\alpha\beta\sin\phi+18(\alpha^4-\beta^4)\cos3\phi+36(\alpha^2+\beta^2)\alpha\beta\sin3\phi\} ,
\end{aligned}$$

(A3a)

$$
\begin{aligned}
d\beta/d\phi = {} & (m/p)\{-(3-\eta)\cos\phi+3\alpha-(5-4\eta)(\alpha\cos2\phi+\beta\sin2\phi) \\
& +\tfrac{1}{8}[(8+21\eta)\alpha^2-(56-47\eta)\beta^2]\cos\phi+\tfrac{1}{4}(32-13\eta)\alpha\beta\sin\phi+\tfrac{3}{8}\eta(\alpha^2-\beta^2)\cos3\phi+\tfrac{3}{4}\eta\alpha\beta\sin3\phi\} \\
& +(m/p)^2\{\tfrac{1}{4}(36+73\eta-8\eta^2)\cos\phi+(7+5\eta-7\eta^2)\alpha+(11+31\eta-3\eta^2)(\alpha\cos2\phi+\beta\sin2\phi) \\
& +\tfrac{1}{16}[(84+79\eta-224\eta^2)\alpha^2+(92+181\eta-32\eta^2)\beta^2]\cos\phi-\tfrac{1}{8}(4+51\eta+96\eta^2)\alpha\beta\sin\phi \\
& +\tfrac{1}{16}(60+245\eta-64\eta^2)[(\alpha^2-\beta^2)\cos3\phi+2\alpha\beta\sin3\phi]-\tfrac{1}{8}(2-21\eta+48\eta^2)\alpha(\alpha^2+\beta^2) \\
& -\tfrac{1}{2}[(3-10\eta+14\eta^2)\alpha^2-(3-11\eta-10\eta^2)\beta^2]\beta\sin2\phi-\tfrac{1}{4}[(\eta+24\eta^2)\alpha^2-(12-43\eta-16\eta^2)\beta^2]\alpha\cos2\phi \\
& +\tfrac{1}{8}(2+25\eta-16\eta^2)[(\alpha^2-3\beta^2)\alpha\cos4\phi+(3\alpha^2-\beta^2)\beta\sin4\phi] \\
& +\tfrac{1}{64}\eta[5(27-41\eta)\alpha^4-6(57+61\eta)\alpha^2\beta^2-(477+161\eta)\beta^4]\cos\phi+\tfrac{1}{16}\eta(153-11\eta)\alpha\beta(\alpha^2+\beta^2)\sin\phi \\
& +\tfrac{3}{128}\eta[(33-19\eta)\alpha^4-6(53+17\eta)\alpha^2\beta^2+(73+53\eta)\beta^4]\cos3\phi \\
& +\tfrac{3}{32}\eta[(43-\eta)\alpha^2-7(9+5\eta)\beta^2]\alpha\beta\sin3\phi \\
& +\tfrac{15}{128}\eta(1-3\eta)[(\alpha^4-6\alpha^2\beta^2+\beta^4)\cos5\phi+4(\alpha^2-\beta^2)\alpha\beta\sin5\phi]\} \\
& -\tfrac{1}{15}\eta(m/p)^{5/2}\{192\sin\phi+304\beta+320(\alpha\sin2\phi-\beta\cos2\phi) \\
& +(230\alpha^2+538\beta^2)\sin\phi+308\alpha\beta\cos\phi+182(\alpha^2-\beta^2)\sin3\phi-364\alpha\beta\cos3\phi \\
& +121\beta(\alpha^2+\beta^2)+10(13\alpha^2+23\beta^2)\alpha\sin2\phi \\
& -20(4\alpha^2+9\beta^2)\beta\cos2\phi+35(\alpha^2-3\beta^2)\alpha\sin4\phi-35(3\alpha^2-\beta^2)\beta\cos4\phi \\
& +6(3\alpha^4+8\alpha^2\beta^2+5\beta^4)\sin\phi+12(\alpha^2+\beta^2)\alpha\beta\cos\phi+18(\alpha^4-\beta^4)\sin3\phi-36(\alpha^2+\beta^2)\alpha\beta\cos3\phi\}\ ,
\end{aligned}
\tag{A3b}
$$

$$
\begin{aligned}
d(p/m)/d\phi = {} & 4(2-\eta)(\alpha\sin\phi-\beta\cos\phi) \\
& +(m/p)\{-2(2+13\eta+2\eta^2)(\alpha\sin\phi-\beta\cos\phi)+\tfrac{1}{2}(4+11\eta)[(\beta^2-\alpha^2)\sin2\phi+2\alpha\beta\cos2\phi] \\
& +\tfrac{1}{4}\eta(33-2\eta)(\alpha^2+\beta^2)(\alpha\sin\phi-\beta\cos\phi)+\tfrac{3}{4}\eta(3+2\eta)[(\alpha^2-3\beta^2)\alpha\sin3\phi-(3\alpha^2-\beta^2)\beta\cos3\phi]\} \\
& -\tfrac{8}{5}\eta(m/p)^{3/2}\{8+18(\alpha\cos\phi+\beta\sin\phi)+7(\alpha^2+\beta^2) \\
& +5[(\alpha^2-\beta^2)\cos2\phi+2\alpha\beta\sin2\phi]+2(\alpha^2+\beta^2)(\alpha\cos\phi+\beta\sin\phi)\}\ .
\end{aligned}
\tag{A3c}
$$

Our goal is to obtain approximate, asymptotic solutions of these equations in the regimes $e \gg u$, and $e \approx u$. Throughout, we assume that $u \ll 1$, and we define the small parameter $\epsilon \approx u$. We then expand α, β, and u in powers of ϵ, according to

$$\alpha \approx \alpha_0+\epsilon\alpha_1+\cdots\ , \tag{A4a}$$

$$\beta \approx \beta_0+\epsilon\beta_1+\cdots\ , \tag{A4b}$$

$$u \approx \epsilon u_0+\epsilon^2 u_1+\cdots\ . \tag{A4c}$$

These quantities are expected to vary over both an orbital time scale described by ϕ, and over a gravitational-radiation-reaction time scale, which is a factor $\epsilon^{-5/2}$ longer. To take these two effects into account, we use a two-scale approach:[33] we define a variable $\theta=\epsilon^{5/2}\phi$, and we assume that α, β, and u depend on both θ and ϕ, now viewed as independent variables. With this assumption, we write

$$d/d\phi=\partial/\partial\phi+\epsilon^{5/2}\partial/\partial\theta\ . \tag{A5}$$

We now substitute Eqs. (A4) and (A5) into (A3), and collect terms of common powers of ϵ. To lowest order, we find

$$\partial\alpha_0/\partial\phi=0,\quad \alpha_0=\alpha_0(\theta)\ , \tag{A6a}$$

$$\partial\beta_0/\partial\phi=0,\quad \beta_0=\beta_0(\theta)\ , \tag{A6b}$$

$$\partial u_0/\partial\phi=0,\quad u_0=u_0(\theta)\ . \tag{A6c}$$

To the next order in ϵ, we find

$$\partial\alpha_1/\partial\phi = u_0\{(3-\eta)\sin\phi - 3\beta_0 + (5-4\eta)(\alpha_0\sin2\phi - \beta_0\cos2\phi) + \tfrac{1}{4}\alpha_0\beta_0[3\eta\cos3\phi - (32-13\eta)\cos\phi] + \tfrac{3}{8}\eta(\beta_0^2-\alpha_0^2)\sin3\phi + \tfrac{1}{8}(56-47\eta)\alpha_0^2\sin\phi - \tfrac{1}{8}(8+21\eta)\beta_0^2\sin\phi\}\,, \tag{A7}$$

with similar equations for β_1 and u_1. Holding the "independent" variable θ fixed, we can integrate these equations to obtain

$$\alpha \approx \alpha_0(\theta) + \epsilon u_0\{-(3-\eta)\cos\phi - 3\beta_0\phi - \tfrac{1}{2}(5-4\eta)(\alpha_0\cos2\phi + \beta_0\sin2\phi) + \tfrac{1}{4}\alpha_0\beta_0[\eta\sin3\phi - (32-13\eta)\sin\phi] - \tfrac{1}{8}\eta(\beta_0^2-\alpha_0^2)\cos3\phi - \tfrac{1}{8}(56-47\eta)\alpha_0^2\cos\phi + \tfrac{1}{8}(8+21\eta)\beta_0^2\cos\phi\}\,. \tag{A8}$$

These solutions could be carried to higher order in ϵ if necessary. However, on the left-hand side of Eq. (A3a), there will occur a term of the form $\epsilon^{5/2}\partial\alpha_0/\partial\theta$, which is purely a function of θ. Matching this with the corresponding purely θ dependent, $\epsilon^{5/2}$ term on the right-hand side, and doing the same for β and u, we obtain the equations

$$\partial\alpha_0/\partial\theta = -(\eta/15)u_0^{5/2}\alpha_0[304+121(\alpha_0^2+\beta_0^2)]\,, \tag{A9a}$$

$$\partial\beta_0/\partial\theta = -(\eta/15)u_0^{5/2}\beta_0[304+121(\alpha_0^2+\beta_0^2)]\,, \tag{A9b}$$

$$\partial u_0/\partial\theta = (8\eta/5)u_0^{7/2}[8+7(\alpha_0^2+\beta_0^2)]\,. \tag{A9c}$$

From the ratio of Eqs. (A9a) and (A9b), we find

$$\alpha_0/\beta_0 = \text{const} \equiv \cot\omega_0\,, \tag{A10}$$

where we now define

$$\alpha_0 \equiv e_0\cos\omega_0\,, \tag{A11a}$$

$$\beta_0 \equiv e_0\sin\omega_0\,. \tag{A11b}$$

Taking the ratio of Eqs. (A9a) and (A9c) and integrating, we find

$$u_0^{-1} = C\alpha_0^{12/19}(304+121\alpha_0^2\sec^2\omega_0)^{870/2299}\,, \tag{A12}$$

where C is an arbitrary constant. With the substitution of Eqs. (A11), we obtain Eq. (3.2). The evolution of these quantities with θ can then be found by completing the integration of Eqs. (A9).

Equations (A12) and (A9c) show that e_0 decreases with θ while u_0 increases with θ, so that eventually $e_0 \approx u_0$. At this stage, we use a different approximation series, given by

$$\alpha \approx \epsilon\alpha_1 + \epsilon^2\alpha_2 + \epsilon^{5/2}\alpha_{5/2} + \cdots\,, \tag{A13a}$$

$$\beta \approx \epsilon\beta_1 + \epsilon^2\beta_2 + \epsilon^{5/2}\beta_{5/2} + \cdots\,, \tag{A13b}$$

$$u \approx \epsilon u_0 + \epsilon^2 u_1 + \cdots\,. \tag{A13c}$$

Substituting these approximations and Eq. (A5) into Eqs. (A3), and collecting powers of ϵ, we obtain, to the lowest order,

$$\partial u_0/\partial\phi = 0,\quad u_0 = u_0(\theta)\,; \tag{A14a}$$

$$\partial\alpha_1/\partial\phi = (3-\eta)u_0\sin\phi\,,\qquad \alpha_1 = -(3-\eta)u_0\cos\phi + \bar{\alpha}(\theta)\,; \tag{A14b}$$

$$\partial\beta_1/\partial\phi = -(3-\eta)u_0\cos\phi\,,\qquad \beta_1 = -(3-\eta)u_0\sin\phi + \bar{\beta}(\theta)\,, \tag{A14c}$$

where $\bar{\alpha}(\theta)$ and $\bar{\beta}(\theta)$ are functions of integration. By comparing these solutions for α and β at order ϵ with Eqs. (A8) in the regime where $\alpha_0 \approx \beta_0 \approx \epsilon$, we find that the solutions match, provided that we identify $\bar{\alpha} = \alpha_0$ and $\bar{\beta} = \beta_0$. Continuing to integrate the equations through $O(\epsilon^{5/2})$, we obtain

$$\alpha \approx \epsilon[-u_0(3-\eta)\cos\phi + \alpha_0(\theta)] + \epsilon^2\{u_0^2(15+\tfrac{17}{4}\eta+2\eta^2)\cos\phi - 3u_0\beta_0(\theta)\phi - \tfrac{1}{2}(5-4\eta)u_0[\alpha_0(\theta)\cos2\phi + \beta_0(\theta)\sin2\phi]\} - \epsilon^{5/2}\tfrac{64}{5}\eta u_0^{5/2}\sin\phi\,, \tag{A15a}$$

$$\beta \approx \epsilon[-u_0(3-\eta)\sin\phi + \beta_0(\theta)] + \epsilon^2\{u_0^2(15+\tfrac{17}{4}\eta+2\eta^2)\sin\phi + 3u_0\alpha_0(\theta)\phi - \tfrac{1}{2}(5-4\eta)u_0[\alpha_0(\theta)\sin2\phi - \beta_0(\theta)\cos2\phi]\} + \epsilon^{5/2}\tfrac{64}{5}\eta u_0^{5/2}\cos\phi\,, \tag{A15b}$$

$$u \approx \epsilon u_0(\theta) + O(\epsilon^3)\,. \tag{A15c}$$

When $(u_i/u_0)^{19/12} \ll u_0 \ll 1$, so that $\alpha_0 \ll u_0$ and $\beta_0 \ll u_0$, we have (dropping the ϵ)

$$\alpha \approx -[(3-\eta)u_0 - (15+\tfrac{17}{4}\eta+2\eta^2)u_0^2]\cos\phi - \tfrac{64}{5}\eta u_0^{5/2}\sin\phi\,, \tag{A16a}$$

$$\beta \approx -[(3-\eta)u_0 - (15+\tfrac{17}{4}\eta+2\eta^2)u_0^2]\sin\phi + \tfrac{64}{5}\eta u_0^{5/2}\cos\phi\,. \tag{A16b}$$

From $e^2 \equiv \alpha^2+\beta^2$ and $\tan\omega \equiv \beta/\alpha$, we obtain the quasicircular solution of Eqs. (A1). In the intermediate regime, where $(u_i/u_0)^{19/12} \approx u_0$, we obtain

$$\alpha \approx \alpha_0 - (3-\eta)u_0\cos\phi + O(u_0^2)\,, \tag{A17a}$$

$$\beta \approx \beta_0 - (3-\eta)u_0\sin\phi + O(u_0^2)\,, \tag{A17b}$$

with the result

$$e^2 \approx e_0^2 + (3-\eta)^2u_0^2 - 2(3-\eta)u_0e_0\cos(\phi-\omega_0)\,, \tag{A18a}$$

$$\omega \approx \omega_0 + \arctan\left[\frac{-(3-\eta)u_0e_0\sin(\phi-\omega_0)}{e_0^2-(3-\eta)u_0e_0\cos(\phi-\omega_0)}\right]\,, \tag{A18b}$$

where $e_0 \approx e_i(u_i/u_0)^{19/12}$. Averaging Eq. (A18a) over $\phi = 2\pi$ gives Eq. (3.14). Figure 6 then illustrates the initial conditions under which the quasicircular orbit of Eqs. (A1) can be reached before the post-Newtonian approximation $u_0 \ll 1$ breaks down.

APPENDIX B: TIDAL DISSIPATION FOR BLACK HOLES

Here we estimate the "effective" mean coefficient of viscosity $\langle \eta \rangle$, used in Eq. (2.21) for tidal dissipation, for the case of black holes. For a slowly rotating black hole in the perturbing gravitational field of a distant, stationary body located on the black hole's equatorial plane, Hartle[34] found that the rate of decrease in angular momentum J of the hole due to tidal dissipation was given by

$$dJ/dt = -\tfrac{8}{5} J m_1^2 m_2^3 / p^6 \ , \qquad \text{(B1)}$$

where m_1 and m_2 are the mass of the body and of the hole, respectively, and $p \gg m_2$ is the separation. We compare this with the general formula for the rate of change of angular momentum of a body due to tidal dissipation: for two bodies in a circular orbit, with the perturbing body having negligible internal angular momentum, so that the total angular momentum $J + J_{\rm orbit}$ is conserved, we have

$$dJ/dt = -dJ_{\rm orbit}/dt = -\tfrac{1}{2}\mu (mp)^{1/2} \dot{p}/p = -\tfrac{1}{3}\mu (mp)^{1/2} \dot{P}/P \ , \qquad \text{(B2)}$$

where μ and m are the reduced and total masses, respectively, and where we have used the fact that $J_{\rm orbit} = \mu (mp)^{1/2}$, $(P/2\pi)^2 = a^3/m$, and $p = a$ for a circular orbit (using Newtonian orbit approximations). Substituting Eq. (2.21) for $\dot{P}/P$, we obtain

$$dJ/dt = -\frac{672\pi}{75} \frac{\mu m m_1}{m_2^3} \frac{R_2^9}{p^6} \langle \eta \rangle (\Omega_2 - n) \ , \qquad \text{(B3)}$$

where $n = 2\pi/P$. For $n \ll \Omega_2$, the distant body can be regarded as almost stationary, so that

$$\Omega_2 - n \approx \Omega_2 \approx J/4m_2^3 \ , \qquad \text{(B4)}$$

where we have assumed a slowly rotating black hole ($J/m_2^2 \ll 1$). Also, for a slowly rotating hole, $R_2 \approx m_2$ (using harmonic coordinates), so that Eq. (B3) becomes

$$dJ/dt = -(168\pi/75) J m_1^2 m_2^4 \langle \eta \rangle / p^6 \ . \qquad \text{(B5)}$$

Comparing this with Eq. (B1), we obtain

$$\langle \eta \rangle \approx 5/7\pi m_2 \ . \qquad \text{(B6)}$$

[1]K. S. Thorne, in *300 Years of Gravitation,* edited by S. W. Hawking and W. Israel (Cambridge University Press, Cambridge, England, 1987), pp. 378–383.

[2](a) B. F. Schutz, Nature (London) **323**, 310 (1986); (b) S. Smith, Phys. Rev. D **36**, 2901 (1987); (c) Y. Gürsel and M. Tinto, *ibid.* **40**, 3884 (1989).

[3]F. J. Dyson, in *Interstellar Communication,* edited by A. G. W. Cameron (Benjamin, New York, 1963), p. 115.

[4]J. P. A. Clark and D. M. Eardley, Astrophys. J. **215**, 311 (1977).

[5]J. M. Lattimer and D. N. Schramm, Astrophys. J. Lett. **192**, L145 (1974); Astrophys. J. **210**, 549 (1976).

[6]J. P. A. Clark, E. P. J. van den Heuvel, and W. Sutantyo, Astron. Astrophys. 72, 120 (1979).

[7](a) S. L. Shapiro and S. A. Teukolsky, Astrophys. J. Lett. **292**, L41 (1985); (b) G. D. Quinlan and S. L. Shapiro, Astrophys. J. **343**, 725 (1989).

[8]J. R. Bond and B. J. Carr, Mon. Not. R. Astron. Soc. **207**, 585 (1984).

[9](a) M. C. Begelman, R. D. Blandford, and M. J. Rees, Nature (London) **287**, 307 (1980); (b) I. H. Redmount and M. J. Rees, Commun. Astrophys. **14**, 165 (1989).

[10]J. H. Taylor and J. M. Weisberg, Astrophys. J. **345**, 434 (1989).

[11]*Frontiers in Numerical Relativity,* edited by C. R. Evans, L. S. Finn, and D. W. Hobill (Cambridge University Press, Cambridge, England, 1989).

[12](a) L. Smarr, in *Sources of Gravitational Radiation,* edited by L. Smarr (Cambridge University Press, Cambridge, England, 1979), p. 245; (b) D. G. Gilden and S. L. Shapiro, Astrophys. J. **287**, 728 (1984).

[13]K. Oohara and T. Nakamura, Prog. Theor. Phys. **82**, 535 (1989); T. Nakamura and K. Oohara, *ibid.* **82**, 1066 (1989).

[14]J. K. Blackburn and S. Detweiler, report (unpublished).

[15]C. W. Misner, K. S. Thorne, and J. A. Wheeler, *Gravitation* (Freeman, San Francisco, 1973), Chap. 39.

[16]For a detailed review, see T. Damour, in *300 Years of Gravitation* (Ref. 1), p. 128.

[17]T. Damour and N. Deruelle, Phys. Lett. **87A**, 81 (1981); T. Damour, C. R. Acad. Sci. Paris **294**, 1355 (1982).

[18]P. M. Fitzpatrick, *Principles of Celestial Mechanics* (Academic, New York, 1970).

[19]R. V. Wagoner and C. M. Will, Astrophys. J. **210**, 764 (1976).

[20]T. Damour and N. Deruelle, C. R. Acad. Sci. Paris **293**, 877 (1981).

[21]T. Damour and N. Deruelle, Ann. Inst. Henri Poincaré A **43**, 107 (1985).

[22]M. Turner and C. M. Will, Astrophys. J. **220**, 1107 (1978).

[23]R. Epstein and R. V. Wagoner, Astrophys. J. **197**, 717 (1975).

[24]L. Blanchet and G. Schäfer, Mon. Not. R. Astron. Soc. **239**, 845 (1989).

[25]Z. Kopal, *Dynamics of Close Binary Systems* (Reidel, Dordrecht, Holland, 1978).

[26]T. G. Cowling, Mon. Not. R. Astron. Soc. **98**, 734 (1938).

[27]A. Krolak, in *Gravitational Wave Data Analysis,* edited by B. F. Schutz (Reidel, Dordrecht, Holland, 1988).

[28]M. E. Alexander, Astrophys. Sp. Sci. **23**, 459 (1973).

[29]P. C. Peters and J. Mathews, Phys. Rev. **131**, 435 (1963).

[30]E. Flowers and N. Itoh, Astrophys. J. **206**, 218 (1976); **230**, 847 (1979).

[31]P. C. Peters, Phys. Rev. **136**, B1224 (1964).

[32]M. Walker and C. M. Will, Phys. Rev. D **19**, 3483 (1979).

[33]C. M. Bender and S. A. Orszag, *Advanced Mathematical Methods for Scientists and Engineers* (McGraw Hill, New York, 1978), Chap. 11.

[34]J. B. Hartle, Phys. Rev. D **8**, 1010 (1973); **9**, 2749 (1974).